EXPRESSION PROFILING AND FUNCTION ELUCIDATION OF ANAPLASTIC LYMPHOMA KINASE IN THE DEVELOPING NERVOUS SYSTEM

by

Shawn Patrick Hurley

A dissertation submitted in partial fulfillment
of the requirements for the degree

of

Doctor of Philosophy

in

Biological Sciences

MONTANA STATE UNIVERSITY
Bozeman, Montana

April 2006

© COPYRIGHT

by

Shawn Patrick Hurley

2006

All Rights Reserved

APPROVAL

of a dissertation submitted by

Shawn Patrick Hurley

This dissertation has been read by each member of the dissertation committee and has been found to be satisfactory regarding content, English usage, format, citations, bibliographic style, and consistency, and is ready for submission to the Division of Graduate Education.

Dr. Frances Lefcort

Approved for the Department of Cell Biology and Neuroscience

Dr. Gwen Jacobs

Approved for the Division of Graduate Education

Dr. Joseph J. Fedock

STATEMENT OF PERMISSION TO USE

In presenting this dissertation in partial fulfillment of the requirements for a doctoral degree at Montana State University, I agree that the Library shall make it available to borrow under rules of the Library. I further agree that copying of this dissertation is allowable only for scholarly purposes, consistent with "fair use" as prescribed in the U.S. Copyright Law. Requests for extensive copying or reproduction of this dissertation should be referred to ProQuest Information and Learning, 300 North Zeeb Road, Ann Arbor, Michigan 48106, to whom I have granted "the exclusive right to reproduce and distribute my dissertation in and from microform along with the non-exclusive right to reproduce and distribute my abstract in any format in whole or in part."

Shawn P. Hurley

April 2006

DEDICATION

This work could not have been accomplished without the opportunity afforded me by my advisor, Dr. Frances Lefcort – thank you for seeing it through with me. I would like to thank my parents, Pat and Jeannie, two of the most humble, loving, supportive and encouraging individuals I have ever known. Without your guidance and words of wisdom, I would not be who I am today. Very special thanks to my grandmothers, Jewel and Betty, and my grandfather Joe in addition to my great-aunts, Joy and Junerose (Dee-Dee), whose words of encouragement have meant everything. In loving memory of Marcella Burke, a true friend and kindred spirit whose love of life and learning has inspired me through the years – I miss you every single day. Warmest thanks for my extended family: Theresa Racicot and Lurie Berry, my second mothers who have kept me in their prayers always, Val, Marta and Lynn – my surrogate sisters who watch out for me here in Bozeman and are three of the most skilled, thoughtful, genuine people I know – and Bob & Lynda Zirpoli, family is just a word, you give it meaning. I could not forget my fellow graduate students, Judy Bononi and Jen Kasemeier-Kulesa, who know the toils of research science and always had a sympathetic ear concerning failed benchwork. To all my former teachers who inspired me to pursue my goals – from Nancy Emmert, my kindergarten teacher who always said I got the best start in her class (and I truly did!), to Tom Pedersen, Ray Hamilton, and Marilyn & Gil Alexander, four very dedicated educators who fostered my pursuits in research – thank you for your tireless hours and the solid educational foundation upon which my current endeavors stand today. Finally, everlasting gratitude to my closest friends, Julie Clay, Mike Heggem, Jennifer Nichols, Nichole and Zarek Pilakowski – I couldn't have made it without you!

TABLE OF CONTENTS

1. INTRODUCTION……...……..1

Receptor Tyrosine Kinases……...…….1
Anaplastic Lymphoma Kinase……...…3
General Organization of the Spinal Cord…….……..……6
Neuronal Specification in the Spinal Cord…….…….…….…….……..…..7
Dorsal/Ventral Polarization……...…7
Motor Neuron Subtype Identity...…….……8
Interneuron Subtype Identity……..……10
Formation and Organization of the Peripheral Nervous System…….……...12
RNA Interference…..……...15
Thesis Objective…..…….18

2. MATERIALS AND METHODS…….19

In Situ Hybridization……...…….……19
Immunohistochemistry…….……20
Limb Ablation……..22
siRNA Design and Synthesis……...23
Construction of shRNA-expressing Plasmids……..24
In Ovo Microinjection and Electroporation…….25
Post-injection Analysis for Loss of Function……...26
Quantitative Analysis……...28

3. RESULTS OF ALK EXPRESSION PROFILING IN CHICK……..…….29

Expression of *Alk* mRNA in the Developing PNS……...29
Expression of *Alk* mRNA in the Spinal Cord…….……..31
Alk Expression in Hind Limb and Body Wall Musculature…..……37
Limb-derived Cues and the Regulation of *Alk*…….……37

4. RESULTS OF ALK KNOCKDOWN IN CHICK SPINAL CORD……...……39

Targeted Silencing of Anaplastic Lymphoma Kinase in Chick Spinal Cord…….……..39
Increased Cell Death in Developing Spinal Cord after *Alk* Knockdown…….42
Identification of Phenotypic Changes in Specific Neuronal Populations……44

5. DISCUSSION……..48

Alk Expression in the Sympathetic Ganglia is Robust and Temporally Extensive……..48
Restricted Expression of *Alk* in the DRG to Mitotically Active Progenitors……..49

TABLE OF CONTENTS – CONTINUED

Alk mRNA is Differentially Expressed in Motor Neuron Subsets and in Muscle Subsets of the Hind Limb and Body Wall……..50
Similar Phenotypic Changes Observed with Use of Different RNAi Methodologies……52
ALK Promotes Cell Survival of Somatic and Visceral Motor Neurons……..53
Future Direction……..……56

6. CONCLUSIONS…….59

LITERATURE CITED……60

APPENDICES……..……71

APPENDIX A: α-ALK ANTIBODY STAINING……..72
Observations……...……..……...73
APPENDIX B: STATISTICAL DATA……..…..…..……74
Statistical Analysis: Student's t-test (one-tailed) – using StatDisk 10.1.0…...……..75

LIST OF TABLES

Table Page

1. Summary of Characteristic HD Protein Expression for Dorsal Interneuron Populations……..11

LIST OF FIGURES

Figure Page

1. Analysis of developmental expression of anaplastic lymphoma kinase (*Alk*) mRNA in chick peripheral nervous system by whole-mount in situ hybridization…….....30

2. Anaplastic lymphoma kinase (*Alk*) mRNA is expressed in mitotically active cells of the dorsal root ganglia (DRG) and sympathetic ganglia (SG)……...……..32

3. *Alk* is dynamically expressed temporally and spatially in the spinal cord……...33

4. *Alk* is expressed by discrete subpopulations of motor neurons…….35

5. Spatial-temporal overview of anaplastic lymphoma kinase (*Alk*) mRNA expression in developing chick nervous system…….36

6. *Alk* is expressed by subsets of hind limb and body wall muscles…….38

7. Schematic representation of shRNA plasmid construction…….....40

8. Cartoon diagram of microinjection and electroporation of nucleic acid in chick neural tube at st 22……...…….40

9. Knockdown of *Alk* transcript in spinal cord is target-specific…….....41

10. *Alk*-specific hairpin constructs lead to increased cell death in chick spinal cord……...43

11. Pre-synthesized *Alk*-specific siRNA leads to increased cell death in chick spinal cord……...…45

12. *Alk* silencing induces premature cell death in somatic motor neurons…….....46

13. Isl1+ thoracic column of Terni motor neurons fail to survive after *Alk* knockdown……...….47

ABSTRACT

During embryonic development, complex events such as cellular proliferation, differentiation, survival, and guidance of axons are orchestrated and regulated by a variety of extracellular signals. Receptor tyrosine kinases mediate many of these events with several playing critical roles in neuronal survival and axonal guidance. It is evident that not all the receptor tyrosine kinases that play key roles in regulating neuronal development have been identified. In these studies, we have characterized the spatial-temporal expression profile of a recently identified receptor tyrosine kinase, anaplastic lymphoma kinase (ALK), in embryonic chick by means of whole mount *in situ* hybridization in conjunction with immunohistochemistry. Our findings reveal that *Alk* is expressed in sympathetic and dorsal root ganglia as early as stage 19. In addition, mRNA is expressed from stage 23/24 (E4) until stage 39 (E13) in discrete motor neuron subsets of chick spinal cord along with a select group of muscles that are innervated by one of these particular motor neuron clusters. Based on these findings, we conducted loss-of-function analyses by means of in ovo RNA interference (RNAi) to determine the role of ALK as it pertains to development of the spinal cord. Results indicate that ALK is involved in the survival of spinal neurons including motor neurons and possibly interneurons. Hence, the data presented here identify ALK as a novel receptor for regulating critical events in the development of the central nervous system and, potentially, the peripheral nervous system.

CHAPTER 1

INTRODUCTION

Extracellular signaling is of crucial importance in the nervous system as it regulates primary developmental events including survival, proliferation, differentiation, migration and patterning. Perhaps the most well-known and best-characterized signaling molecules in the nervous system are the neurotrophins. These trophic factors comprise a family of proteins that mediate growth, differentiation, and survival of different classes of neurons (Kaplan & Miller, 2000). The complementary components to these growth factors are their receptors, the Trk tyrosine kinases and the p75 neurotrophin receptor, with Trk receptors belonging to a superfamily of proteins known as receptor tyrosine kinases (RTKs).

Receptor Tyrosine Kinases

Over the past decade, cell-to-cell signaling has become an expansive area of study with the discovery of a wide variety of cell-surface receptors. One such set of receptors that has become of particular interest is the receptor tyrosine kinase (RTK) superfamily. RTKs are characterized as membrane spanning receptors possessing an extracellular ligand-binding domain (ECD) which is usually glycosylated, a hydrophobic transmembrane domain, and an intracellular domain consisting of a juxtamembrane region, followed by the tyrosine kinase catalytic domain and a carboxy-terminal region (Hubbard & Till, 2000). The overall architecture of the tyrosine kinase domain is a bi-lobed structure composed of an amino-terminal (or upper) lobe, containing a five-stranded β sheet and one α helix, and a carboxy-

terminal (or lower) lobe that is mainly α-helical (Hubbard & Till, 2000). A majority of the RTKs are monomeric and will dimerize upon binding of ligand (Schlessinger, 2000). Ligand-induced dimerization facilitates full kinase/receptor activation which occurs in two steps: 1) enhancement of inherent catalytic activity and 2) subsequent phosphorylation of tyrosine residues within the receptor's cytoplasmic domain including the juxtamembrane, kinase insert, and carboxy-terminus (Hubbard & Till, 2000). Regarding this first step, enhanced kinase activity is necessary for subsequent phosphorylation of protein substrates and is controlled through modulation of the catalytic site by means of phosphorylating residues in the activation loop. At the molecular level, this process begins when ATP binds to a nucleotide-binding loop in the cleft between the two lobes of the kinase domain. This loop contains a highly conserved motif, GXGXXG followed by AXK ~20 residues downstream. The GXGXXG binds to ATP while the invariant lysine residue (K) stabilizes the substrate-binding cleft by means of electrostatic interactions with a glutamate residue. ATP is now in position to transfer its γ-phosphate to the protein substrate. Normally, there is an autoinhibition of the catalytic site due to steric interference of the activation loop. In the case of the insulin receptor, a tyrosine (unphosphorylated) near the beginning of the activation loop is bound in the active site, hydrogen-bonded to a conserved aspartate and arginine in the catalytic loop. It appears that this tyrosine competes with neighboring β chains and exogenous proteins substrates for the active site thus limiting the kinase activity of the receptor. When trans-autophosphorylation (phosphorylation from the other receptor brought in close proximity due to dimerization) of this tyrosine occurs, the p-Tyr residue leaves the active site and enzymatic activity is restored. As a result, further tyrosines within

the receptor can now be phosphorylated, providing docking sites for modular domains such as SH2 (Src Homology Region 2) and PTB (Phosphotyrosine Binding) found in adapter proteins that serve to propagate signal cascades.

Multiple members of the RTK family are expressed in the developing central and peripheral nervous systems (CNS, PNS) where they regulate such key events as growth, cell proliferation, differentiation, cell survival, and synaptogenesis (Schlessinger, 2000). In particular, RTKs play a critical role in promoting the survival of neurons from populations in which a large number undergo programmed cell death (PCD) during target innervation (Huang and Reichardt, 2001). Even with the discovery of numerous survival-promoting neurotrophins, the application of these ligands, individually or in concert, fails to save all motor neurons (MNs) from death; conversely, removal of specific neurotrophins or the RTKs through which they signal results in no greater than 40% PCD in MNs not originally intended to die (Gould and Oppenheim, 2004). This suggests that not all the factors that mediate motor neuron survival have yet been identified. Thus, further identification of additional RTKs that play key roles in regulating neuronal development is still needed.

Anaplastic Lymphoma Kinase

Anaplastic lymphoma kinase (ALK) is a recently identified RTK whose function *in vivo* remains speculative. ALK was originally identified as an oncogenic manifestation in anaplastic large cell lymphomas (ALCL) (Shiota et al., 1994). This non-Hodgkin's lymphoma has been attributed to a t(2;5) chromosomal translocation resulting in a nucleophosmin (NPM)-ALK fusion protein, known as p80 and composed of the amino

portion of NPM and the intracellular carboxy portion of ALK, which gives rise to constitutively activated ALK signaling (Pulford et al., 2004). Identification of normal full-length human ALK revealed a single-pass transmembrane RTK belonging to the insulin receptor subfamily (Morris et al., 1997). Previous studies in mice have demonstrated an expression profile restricted to discrete areas of the developing CNS and PNS (Iwahara et al., 1997; Morris et al., 1997). In *Drosophila*, ALK is expressed in the developing CNS and is also involved in visceral mesoderm differentiation (Lee et al., 2003; Loren et al., 2003; Loren et al., 2001). ALK has also been identified in *C. elegans* where it is expressed at low levels in the nervous system and is proposed to inhibit or destabilize synapse differentiation (Liao et al., 2004). While these papers do not specifically address the function(s) of ALK, its conserved expression within the CNS suggests an important role(s) in neural development.

Investigations regarding the physiological function of mammalian ALK have yielded intriguing yet varied results. Chimeric fusions of ALK were among the first engineering attempts, in which the extracellular domain (ECD) of ALK was replaced with the IgG 2b Fc or epidermal growth factor receptor (EGFR) domain, to create a chimeric receptor that could dimerize and activate ALK signaling (Souttou et al., 2001). In the case of the ALK.Fc chimera, PC12 cells expressing the fusion protein underwent neurite outgrowth indicating ALK's potential involvement in neuronal differentiation (Souttou et al., 2001). Transfection of the EGFR/ALK hybrid into NIH3T3 cells followed by administration of epidermal growth factor (EGF) induced cell transformation suggesting a role for ALK in cell proliferation (Piccinini et al., 2002).

Two growth factors, pleiotrophin (PTN) and midkine (MK), have been identified as potential ligands for the ALK receptor (Stoica et al., 2001; Stoica et al., 2002). Both factors are secreted, heparin-binding proteins with PTN 55% homologous to MK. Concerning chick, *Ptn* is expressed in dorsal and ventral spinal cord, DRG, and developing hind limb from stage 23 until at least stage 37 (Nolo et al., 1996; Dreyfus et al., 1998). In *Drosophila*, the expression profile of PTN/MK protein family homologs, *miple1* and *miple2*, complements the expression pattern of the *Alk* homolog. As previously mentioned, *Drosophila Alk* is expressed in visceral mesoderm which is in contact with endoderm, expressing *miple2*. *Alk* is also expressed in Drosophila's CNS, coinciding with high expression levels of *miple1* (Englund et al., 2006). Interactions of PTN and MK with ALK in fibroblast, adrenal carcinoma, neuroblastoma and glioblastoma cell lines stimulated anti-apoptotic signaling and promoted cell survival (Bowden et al., 2002; Powers et al., 2002; Stoica et al., 2002). While PTN and MK have a demonstrated affinity for ALK in vitro, they also bind receptor protein tyrosine phosphatase-ζ/β (RPTP-ζ/β) (Maeda et al., 1999; Maeda et al., 1996) and syndecans (heparin sulfate proteoglycans) (Kojima et al., 1996). Hypothetically, syndecans may serve as accessory molecules for PTN/MK presentation in cells adjacent to ALK-bearing cells or allow for PTN and MK to associate with extracellular matrix. Such interplay is supported by the fact that for the fibroblast growth factor family initial binding to proteoglycans may be required for presentation to their signal-transducing receptors (which are also RTKs) (Elenius and Jalkanen, 1994). Motegi and colleagues (2004) developed an agonist monoclonal antibody against the ECD of human ALK in order to solely investigate ALK-mediated activity. Their results indicated that ALK transmits both

mitogenic and differentiation signals in SK-N-SH human neuroblastoma cells (Motegi et al., 2004).

Because of its potential importance, coupled to the extensive characterization of embryonic spinal cord and PNS, determination of ALK's function in the developing nervous system will be extremely insightful. Given the ease of manipulations in ovo, the chick affords an excellent model system for functional assessment of ALK in vivo. However, a full-length cDNA for *Alk* has not been identified and sequenced yet in chick. This makes functional analyses via loss-of-function and gain-of-function experimentation problematic since neither dominant negative nor full-length forms of ALK can be cloned and overexpressed. Still, loss-of-function assays are possible via silencing of gene expression through ribonucleic acid interference (RNAi). In ovo RNAi in chick embryos is an alternative tool that can provide evidence of a gene's function in vivo without the need for full-length cloning of a candidate gene (Pekarik et al., 2003). Thus RNAi provides a feasible approach for the evaluation of ALK in chick.

General Organization of the Spinal Cord

Upon its genesis, a layer of rapidly dividing neural stem cells, one cell layer thick and known as germinal neuroepithelium, comprises the newly formed neural tube. This progenitor germ layer is mitotically active and yields progeny cells that migrate to form a second layer surrounding the original neural tube. As more and more cells are added to this new layer, it becomes increasingly thicker and known as the mantle zone with the germinal epithelium now called the ventricular zone.

Cells of the mantle zone differentiate into spinal neurons and glia – these neurons project axons away from the lumen of the cord, creating a third layer, the marginal zone, that is relatively free of cell bodies. Over time, glial cells ensheath the axons in the marginal zone with myelin, imparting a whitish color to this area. Thus the axonal marginal layer is often referred to as the white matter of the spinal cord whereas the mantle zone, containing darker neuronal cell bodies, is frequently called the gray matter.

Neuronal Specification in the Spinal Cord

Dorsal/Ventral Polarization

Shortly after closure of the neural tube, bone morphogenic protein-4 (BMP-4) and bone morphogenic protein-7 (BMP-7), both members of the transforming growth factor-β (TGF-β) family, are secreted from dorsally adjacent epidermal ectoderm while sonic hedgehog (Shh) protein has been expressed since the neural fold stage from the ventally-positioned notochord. These paracrine factors establish secondary signaling centers by inducing the apical and basal portions of the neuroepithelium to become the roof plate and floor plate respectively.

The cells of the floor plate now release Shh that diffuses dorsally through the neural tube and creates a gradient where the concentration of secreted Shh progressively decreases in regions lying more dorsal to this ventral expression center (Roelink et al., 1995; Briscoe et al., 1999). Counterpart to the floor plate, induced roof plate cells produce BMP-4 which initiates a cascade of TGF-β proteins, including BMP-4, BMP-7, BMP-5, dorsalin, and activin, in adjacent cells (Liem et al., 1997). Similar to Shh emanation from the floor plate, a

concentration gradient is generated as TGF-β factors diffuse from the roof plate; however, these factors spread ventrally into the neural tube rather than dorsally.

These secondary signaling centers lead to the compartmentalization of progenitor domains along the dorsal/ventral axis of the ventricular zone by means of transcription factor expression. For example, in the ventral half of the neural tube, Class I progenitor factors are repressed by Shh, and Class II progenitor factors are activated by Shh. The graded Shh diffusion in ventral neural tube results in unique combinations of activated/repressed transcription factors that identify five progenitor domains: p3, pMN, p2, p1, and p0. V0 – V3 interneurons develop from the p0 – p3 domains, respectively, and motor neurons (MNs) arise from the pMN domain (Lee and Pfaff, 2001). As postmitotic cells emerge from the progenitor domains, in both dorsal and ventral halves of the spinal cord, they begin to express new sets of transcription factors that contribute to the identity of distinct neuronal subtypes.

Motor Neuron Subtype Identity

Although all motor neurons (MNs) originate from a single progenitor domain in the ventral neural tube, there exist five orders of distinction for identification of postmitotic motor neurons and their subtypes. These classifications are based on axonal projection, spatial orientation within the spinal cord, and/or use of transcription factors as molecular markers (Jessell, 2000).

First is a generic classification of a spinal neuron as a motor neuron based on axonal projection outside of the spinal cord (interneurons and their axons are housed entirely within

the confines of the spinal cord). Second is recognition of the class to which a motor neuron belongs, visceral or somatic, identifiable by target innervation – skeletal muscle for somatic motor neurons and neuronal or glandular targets for visceral motor neurons. Thirdly, a division can be made among motor neurons based on columnar organization in which longitudinal grouping of motor neurons are present at different rostrocaudal levels of the spinal cord. Motor neurons of the medial motor column (MMC) are present all along the anterioposterior axis, but motor neurons of the lateral motor column (LMC) are restricted to limb levels. In addition, there are groups of visceral motor neurons present in the thoracic and sacral regions known as the sympathetic preganglionic motor column (PMC) or column of Terni (CT) and parasympathetic PMC or CT, respectively, in chick. Motor neurons from these columns are positioned more dorsal-medially, near the central canal, and express only Isl1 (Oppenheim et al., 1982a; Prasad and Hollyday, 1991; Shirasaki and Pfaff, 2002). A further division of each column (with the exception of the CT) into a medial and lateral portion constitutes a fourth order of distinction. The medial portion of the MMC is present at all axial levels, projects axons to axial muscles, and expresses Isl1, Isl2, and Lim3 transcription factors as molecular markers. Motor neurons of the lateral MMC, however, are present only in the thoracic region, extend axons to body wall musculature, and express just Isl1 and Isl2 (Shirasaki and Pfaff, 2002). Medial LMC motor neurons innervate ventrally derived limb muscles and express Isl1 and Isl2, whereas lateral LMC motor neurons innervate dorsally derived limb musculature and express Lim1 and Isl2 (Landmesser, 2001; Shirasaki and Pfaff, 2002). Lastly, motor neurons may be identified as subsets of discrete spatial clusters, known as motor pools, within the LMC that innervate a specific muscle

(Hollyday, 1980; Landmesser, 1978). Certain motor pools are identifiable based on motor neuron expression of particular members of the ETS protein family (Lin et al., 1998).

Interneuron Subtype Identity

Designated as one of two general classifications, commissural or association, interneurons relay sensory information, coordinate activity at different spinal levels, and modulate motor neuron activity. Specifically, commissural interneurons extend axons to the contralateral side of the spinal cord and play an important role in the coordination of left/right alternation during locomotion. Association interneurons form connecting links between sensory and motor neurons and/or other association neurons, serving to integrate sensory input and complete neural circuitry.

Interneurons comprise the majority of neurons in the spinal cord with twelve distinct subtypes. Eight of these populations are dorsally derived while the remaining four originate from progenitor domains within the ventral portion of the ventricular zone. Dorsal progenitor domains are distinguishable from ventral domains by the expression of basic helix-loop-helix (bHLH) transcription factors opposed to homeodomain (HD) transcription factors that are characteristically expressed by the latter domains (Zhuang and Sockanathan, 2006).

Dorsal interneurons (dI) are divided into six early born (dI1 – dI6) and two late born (dIL^{A} and dIL^{B}) subtypes based on birthdate, dorsoventral positioning, and HD protein expression (Table 1) (Zhuang and Sockanathan, 2006). The dI are further subdivided into two groupings, Class A (dI1 – dI3) and Class B neurons (dI4 – dI6 and $dIL^{A/B}$).

Dorsal Interneuron Population	**HD Protein Expression Profile**
dI1	Lh2a/b, Brn3a
dI2	Lim1/2, Brn3a
dI3	Isl1/2, Brn3a
dI4	Lbx1, Lim1/2, Pax2
dI5	Lbx1, Lmx1b, Brn3a
dI6	Lbx1, Lim1/2, Pax2
dIL^{A}	Lbx1, Lim1/2, Pax2
dIL^{B}	Lbx1, Lmx1b, Brn3a

Table 1. Summary of characteristic HD protein expression for dorsal interneuron populations (Helms and Johnson, 2003).

Class A interneurons rely on roof plate-derived signals, such as TGF-β family members (BMP-4, -5, -7, dorsalin, and activin) and wingless-related mouse mammary tumor virus integration site proteins (Wnt1 and Wnt3a), for their development (Zhuang and Sockanathan, 2006). However, Class B neurons are generated independently of roof plate signal influence. It has been proposed that retinoic acid may mediate development of Class B populations since it is required for the generation and specification of V0 and V1 ventral interneurons which neighbor Class B interneurons (Zhuang and Sockanathan, 2006).

Ventral interneurons are divided into four distinct populations (V0 – V3) based on dorsoventral positioning and expression profiles of transcription factors. V0 neurons are identifiable by Evx1 (Moran-Rivard et al., 2001), V1 cells by En1 (Saueressig et al., 1999), V2 interneurons by Lim3 (Ericson et al., 1997; Sharma et al., 1998; Tanabe et al., 1998) and

Chx10 (Ericson et al., 1997; Tanabe et al., 1998), and V3 neurons by Sim1 (Ericson et al., 1997).

Formation and Organization of the Peripheral Nervous System

The vertebrate neural crest is a transient population of precursor cells that generates many derivatives including neurons, melanocytes, skeletal elements, and glia (Krull, 2001). Neural crest cells arise in and begin migration from the dorsal neural tube shortly after fusion of the neural folds and neural tube closure (Ranscht and Bronner-Fraser, 1991).

There are three types of neural crest cells based on body region location including cranial (cephalic), cardiac, and trunk neural crest. Cranial neural crest differentiate into cartilage, bone, cranial neurons, glia, and connective tissue of the face. Cardiac neural crest, which is the caudal region of the cranial neural crest, generate the endothelium of the aortic arteries and the septum between the aorta and the pulmonary artery. Lastly, trunk neural crest cells will give rise to neurons, peripheral glia (including myelinating and non-myelinating Schwann cells, satellite cells, and enteric glia), melanocytes, and chromaffin cells of the adrenal medulla. Due to the interest in neural crest as it pertains to the eventual establishment of the peripheral nervous system, further discussion of events will focus on the trunk neural crest.

Formation and migration of neural crest cells from the neural folds is initiated via interactions of the neural plate with presumptive epidermis, resulting in exposure of pre-neural crest cells to BMP-4 and BMP-7 in the presence of Wnt and FGF proteins (LaBonne

and Bronner-Frasser, 1998). As neural crest delaminate from the neural tube, they undergo an epithelial-to-mesenchyme transformation; without the expression of certain factors, such as Slug protein, induced by BMPs, neural crest cells would fail to emigrate from the neural tube (Nieto et al., 1994).

Neural crest migration occurs in a stereotypic manner along two pathways, ventromedial and dorsolateral, until their final destination is reached. Once somites mature, compartmentalizing into the epithelial dermamyotome and the mesenchymal sclerotome, ventromedial migration and invasion of neural crest cells begin (Krull, 2001). The ventromedial route passes through the somitic mesoderm, or sclerotome, and dorsolateral migration takes place between the somites and overlying ectoderm (Krull, 2001). Neural crest cells along the ventromedial path give rise to neurons, Schwann cells, and chromaffin cells with those that remain in the sclerotome becoming the dorsal root ganglia (DRG), and those that continue more ventrally becoming the sympathetic ganglia and the adrenal medulla (Le Douarin and Teillet, 1974). Interestingly, cells that will populate the sympathetic ganglia are the first to migrate from the trunk neural tube and travel ventrally until they reach positions adjacent to the dorsal aorta where the primary sympathetic chain will be established. Secreted BMP-4, from the dorsal aorta, interacts locally with these cells to promote their maturation into sympathetic neurons (Reissmann et al., 1996; Schneider at al., 1999). Once the primary sympathetic ganglia chain has formed on either side of the dorsal aorta, a dorsolateral migration of these cells (24 hours later) ensues (Tello, 1925; Kirby and Gilmore, 1976) that will result in formation of the secondary sympathetic chain with a final position lying immediately ventral to the DRG (Cornbrooks et al., 1997).

With further regard to migration ventromedially, neural crest cells enter the rostral half of the sclerotome, but not the caudal, causing neural crest cells to be segmented in the somitic mesoderm (Rickmann et al., 1985). This phenomenon contributes to the overall segmental organization of the peripheral nervous system (Goldstein and Kalcheim, 1991). This restricted entry is a result of the combination of positive guidance cues, located in the rostral half of the sclerotome, and negative guidance cues, located in the dermamyotome and caudal portion of the sclerotome. Examples of these guidance cues include: ephrin interactions with Eph receptors (receptor tyrosine kinase family member) (Wang and Anderson, 1997; Krull et al., 1997; McLennan and Krull, 2002), Slit2 interactions with Robo1/2 receptors, Sema3A (Shepherd et al, 1996; Eickholt et al., 1999), peanut agglutinin (PNA)-binding glycoproteins (Krull et al., 1995), F-spondin (Debby-Brafman et al., 1999), and neuregulin interactions with the RTK ErbB family (Britsch et al., 1998).

An additional point of interest is that ventromedial precedes dorsolateral migration by about 24 hours due to the fact that inhibitory factors, such as PNA-binding glycoproteins and chondroitin-6-sulfate, are expressed on the dorsolateral path (Krull, 2001). Ablation of PNA-binding glycoproteins and chondroitin-6-sulfate allow premature entrance of cells along the dorsolateral path. After 24 hours, inhibitors are downregulated, a simultaneous entry of neural crest cells is observed (Krull, 2001), and cells taking the dorsolateral pathway yield melanocytes.

RNA Interference

Silencing of gene expression was first observed over fifteen years ago in plants where the phenomenon was termed posttranscriptional gene silencing (PTGS) (Napoli et al., 1990; Smith et al., 1990; van der Krol et al., 1990). Upon further investigation, a 25 nucleotide RNA species, corresponding to both the sense and antisense sequence of mRNA from silenced genes, was discovered and found to temporally coincide with the onset of PTGS (Hamilton and Baulcombe, 1999). The accumulation of these 25-mers suggested an important role of double-stranded RNA (dsRNA) in triggering PTGS. The term RNA interference (RNAi) was first coined when dsRNA injection in *C. elegans* led to silencing of genes highly homologous to the delivered nucleic acid (Fire et al., 1998) – duplexed RNA now had been shown to be the potent inducer of gene silencing. Since that time, RNAi has been observed in additional organisms such as the fungus, *Neurospora crassa* (where the phenomenon is known as quelling), *Drosophila*, fish, avians, and mammals. It has been proposed that PTGS is evolutionarily conserved as it serves to defend a genome against molecular parasites such as viruses and transposons while removing abundant but aberrant nonfunctional mRNAs (Tijsterman et al., 2002).

While the specific molecular mechanisms of RNAi have yet to be delineated, there are identifiable factors associated with RNAi that have led to the current model of how RNAi works. First, dsRNA is enzymatically digested into 21-23 nucleotide fragments known as short or small interfering RNAs (siRNAs). Cleavage is carried out in an ATP-dependent fashion by an RNase III family member identified as Dicer. Next, the siRNAs associate with

an enzyme complex, RNA-induced silencing complex (RISC), which possesses helicase and endonuclease activity distinct from that of Dicer. Upon unwinding of the siRNA duplex, the antisense strand guides the complex to the target mRNA by base-pairing with recognizable complementary sequence. Transcript is then degraded leading to effective silencing of gene expression.

In an endeavor to circumvent the need of long dsRNA, Tuschl et al. (1999) first injected short RNA duplexes that mimicked Dicer products in vitro. They and others demonstrated that it was possible to directly trigger RNA interference through the introduction of chemically synthesized siRNAs (Caplen et al., 2001; Elbashir et al., 2001). These efforts have led to the current widespread use of commercially available technologies for the introduction of siRNA in vitro or in vivo. In addition to direct chemical synthesis of siRNAs, it also has been shown that short hairpin RNAs (shRNAs) (which are processed by Dicer to become siRNAs through excision of the intervening loop sequence) induce sequence-specific gene silencing (Paddison et al., 2002). A distinct advantage of shRNAs is the ability to endogenously synthesize these molecules in cells transfected with a pol III expression plasmid containing the hairpin sequence. This vector-based approach offers longer-term suppression of gene function due to the renewable source of siRNAs. SiRNA and shRNA-based methodologies have proven even more useful as larger dsRNA molecules can result in antiviral responses such as nonspecific RNA degradation (categorized as an off-target event) (Minks et al., 1979).

The desired use of these RNAi techniques for loss-of-function analyses has led to areas of study devoted to accurately predicting the efficacy of transcript ablation for

candidate siRNA and shRNA sequences. Reynolds and colleagues (2004) designed an algorithm using sequence characteristics of specific residues found to correlate with siRNA potency. Several additional studies have followed with varying results, making the issue of which criteria will portend an efficacious siRNA somewhat controversial (Taxman et al., 2006). While algorithmic prediction remains questionable, thermodynamic properties of siRNAs appear to play a critical role in determining function and strand retention by the RNA-induced silencing complex – functional duplexes display a lower internal stability at the 5' antisense end than nonfunctional duplexes (Khvorova et al., 2003). Still, attempts to anticipate the best siRNA or shRNA sequence that will be the most potent gene silencer are not always successful. Currently, the most prudent course of action is to select several targeting sequences with low internal thermodynamic stability and empirically determine the knockdown capabilities of each.

The chick is becoming an increasingly preferred vertebrate model in which RNAi-mediated knockdown studies can be conducted. Several reasons exist for the increasing use of chick: 1) the relatively low cost of embryos in large numbers, 2) the evolutionary similarities of birds and mammals, 3) the accessibility to all stages of the embryo, and 4) the effective introduction of nucleic acid molecules into chick through in ovo electroporation. Recent studies also demonstrate the effectiveness and success of shRNA plasmids and chemically synthesized siRNAs regarding functional knockdown of gene transcripts in chick (Bron et al., 2004; Chesnutt and Niswander, 2004; Rao et al., 2004; Rao and Sockanathan, 2005).

Thesis Objective

The focus of this thesis concerns the determination of where/when *Alk* is expressed in embryonic chick and the elucidation of an in vivo function for the receptor. Based on our transcriptional profiling via whole-mount in situ hybridization, we utilized techniques in RNAi, including in ovo electroporation of shRNA plasmids and siRNAs, to investigate ALK's potential involvement in spinal neuron cell survival.

CHAPTER 2

MATERIALS AND METHODS

In Situ Hybridization

Fertilized White Leghorn chicken eggs were obtained from SPAFAS (Charles River) and incubated at 37°C on mechanized inclined racks that slowly raise and lower the eggs, creating a simulated "rocking" motion. Embryos were dissected and staged according to Hamburger and Hamilton (Hamburger and Hamilton, 1992). Chick embryos from a range of selected stages, including 19, 22, 23, 24, 25, 35, and 39, were fixed in 4% paraformaldehyde in 1X phosphate buffered saline, pH 7.4 (PBS), and subjected to whole-mount *in situ* hybridization (Nieto et al., 1996; Wilkinson and Nieto, 1993). Briefly, two separate digoxygenin-labeled antisense riboprobes were generated, one targeting a portion of ALK's intracellular domain sequence (~800 n.t. – corresponding to nucleotides 3720-4527 in human ALK; NCBI accession no. NM_004304) and one targeting a region within the extracellular domain sequence (~700 n.t. – corresponding to nucleotides 2043-2714 in human ALK; NCBI accession no. NM_004304). The riboprobe targeting the intracellular portion was derived from a cloned fragment of *Alk* cDNA (provided by Dr. Douglas Clary, Sugen) obtained during a partial library screen using st 35 chick spinal cord. The extracellular domain probe was synthesized from a cloned fragment of *Alk* cDNA generated via RT-PCR using total RNA from st 25 chick spinal cord. Primers were designed using available predicted chicken ALK sequence from the Ensembl database (www.ensembl.org/Gallus_gallus) (forward 5′-ACTGGCTGTTCACAACATGTGGTG-3′, reverse 5′-GATCTTCCTCCAGTAGCACCT-

TCCAG-3′). Expression patterns obtained for the two probes were identical, and sense-control riboprobes yielded no overlapping signal. Embryos were dehydrated in a series of graded methanol washes for 15 min each (25%, 50%, 75%, and 100% in PBS, pH 7.4, containing 0.25% Tween-20 (PBST)) and then re-hydrated by performing the methanol washes in reverse. After 1h incubation in 6% H_2O_2 followed by proteinase K (10 ug/mL) treatment, cRNA digoxygenin-labeled probes were hybridized in 50% foramide/5X SSC, pH 4.5/50 μg/mL heparin/50 μg/mL yeast tRNA at 70°C overnight. After hybridization, embryos were washed three times in 50% formamide/5X SSC, pH 4.5/1% SDS for 30 min at 70°C, three times in Tris buffered saline, pH 7.5 (TBS), with 0.25% Tween-20 for 5 min at room temperature, three times in 50% formamide/2X SSC, pH 4.5, for 30 min at 60°C, and blocked in 10% normal goat serum (NGS) in TBS, pH 7.5, containing 0.1% Tween-20 (TBST) for 90 min at room temperature. Detection of probe hybridization was achieved with α-digoxygenin-AP antibody (Roche, Indianapolis, IN; 1 093 274) (1:3000) in 1% NGS in TBST at 4°C overnight and subsequent incubation with the chromogenic substrate, nitro-blue tetrazolium/5-bromo-4-chloro-3-indolyl phosphate (NBT/BCIP) (prepared solution, Sigma-Aldrich, St. Louis, MO; B-1911). All embryos were then post-fixed in 3.7% formaldehyde and prepared for either cryosectioning or vibratome slicing.

Immunohistochemistry

Following *in situ* hybridization (without Proteinase K treatment), embryos were embedded in either optimal cutting temperature (OCT) compound (Tissue-Tek) when cryosectioning or

5% agarose/8% sucrose-PBS when vibratome-sectioning and then sectioned (14 μm for cryosections, 100 μm for vibratome slices). Stage 25 embryo slide-mounted cryosections were blocked with 10% NGS in TBS, pH 7.5, for 1h at room temperature and incubated overnight at 4°C with α-Isl1 or α-Lim1/2 primary antibody (1:10) in 0.4% Triton-X and 10% NGS in TBS, pH 7.5. Isl1 monoclonal antibody (Developmental Studies Hybridoma Bank, University of Iowa, Iowa City, IA; 40-2D6) was raised in mouse against residues 86-175 of chicken Isl1 expressed in *E. coli*. The antibody has been well characterized for its recognition of the transcription factor in MNs within the medial portion of the lateral motor column (Tsuchida et al., 1994). Lim1/2 monoclonal antibody (Developmental Studies Hybridoma Bank, University of Iowa, Iowa City, IA; 4F2) was raised in mouse against residues 1-360 of rat Lim2 expressed in *E. coli*. The antibody has been well characterized for its identification of Lim1 in MNs within the lateral portion of the lateral motor column (Tsuchida et al., 1994). Slides were rinsed four times in 10% NGS and incubated for 1h at room temperature with a biotinylated goat anti-mouse IgG secondary antibody (Vector, Burlingame, CA; BA-9200) (1:600) followed by fluorescein avidin (Vector, Burlingame, CA; A-2011) (1:600) for 1h at room temperature, rinsed, and mounted in Prolong Anti-fade (Molecular Probes, Eugene, OR; P-7481). Stage 23 embryo vibratome slices were blocked in 10% NGS for 2h at 4°C and incubated overnight at 4°C with α-Tuj1 (1:1000) and α-phoso-histone H3 (1:750) or α-Isl1 (1:10) and α-phospho-histone H3 (1:750) primary antibodies in 0.4% Triton-X and 10% NGS. Tuj1 monoclonal antibody (Berkeley Antibody Company, Berkeley, CA; MMS-435P) was raised in mouse against rat microtubules (peptide epitope, CEAQGPK). It is well characterized for recognition of neuron specific Class III β-tubulin

(Lee et al., 1990). H3 polyclonal antibody (Upstate, Charlottesville, VA; 06-570) was raised in rabbit against an N-terminal peptide (ARKpSTGGKAPRKQL) corresponding to amino acids 8-21 of chicken histone H3. The antibody has been characterized as a mitosis marker, recognizing phosphorylated histone H3 (Rifkin et al., 2000). Slices were washed six times in 10% NGS for 10 min and incubated for 2h at room temperature with goat anti-mouse IgG alexafluor 568 and goat anti-rabbit IgG alexafluor 488 secondary antibodies (Molecular Probes, Eugene, OR; A-11004 & A-11008, respectively) (1:2000), rinsed, and mounted in Prolong Anti-fade.

Whole-mount images were captured using Axiovision 3.1 software (Zeiss) in conjunction with an AxioCam HRC digital video camera (Zeiss). *In situ* hybridization and immunohistology sections were photographed using Kodak Elite Chrome 100 (fine grain) color slide film and a 35 mm camera (Nikon FX-35DX) attached to a Nikon Microphot-FXA fluorescence scope via the phototube assembly. Digital images of color slides were acquired using a Nikon Super Coolscan 4000 slide scanner and accompanying Nikon Scan software. Adobe Photoshop 7.0.1 was utilized to convert whole-mount images to black and white, uniformly modify image size for each photomicrograph within a figure, and to adjust image background color to near-white using the selective color adjustment function.

Limb Ablation

One-sided limb ablations were performed on chick hind limb buds at stage 17/18. Briefly, eggs were placed on their sides and a portion of each shell was cut away to expose and provide access to the developing embryo. A 5% solution of India ink was injected

underneath the embryo to help visualize the location of limb buds. Once a hind limb bud had been identified, a pair of fine-tipped dissection forceps was used to clip and excise the prospective limb. After the surgical procedure, eggs were sealed with tape, and embryos were allowed to develop to stage 23/24 followed by *in situ* hybridization to determine impact upon *Alk* expression.

siRNA Design and Synthesis

Candidate target sequences for *Alk* were identified using the resources of Dharmacon, Inc. (www.dharmacon.com). 5′-incomplete predicted chick *Alk* sequence from the Ensembl database (www.ensembl.org/Gallus_gallus; gene ID: ENSGALG00000009034) was analyzed with the aid of the "siDESIGN Center" tool. Employing an algorithm designed by Reynolds et al. (2004), the design tool identified eleven siRNA sequences after BLAST analysis. Two of the siRNAs scored a "9" out of a possible "10" with the remaining sequences scoring "8." One of the target sequences, achieving a "9" and possessing a GC content of 31.6%, was selected and once again subjected to BLAST searches using GenBank's nonredundant (nr) and EST databases to ensure the siRNA's specificity for *Alk*. With the identification of no off-target gene recognition, the candidate siRNA was deemed acceptable. To confirm that *Alk* gene silencing was not triggered by unrelated siRNAs, an siRNA targeting the fluorescent reporter DsRed was used as a negative control (Rao et al., 2004; Rao and Sockanathan, 2005). RNA duplexes were ordered in 2′ deprotected, annealed, and desalted form (Option A4) from Dharmacon, Inc. Upon receipt, lyophilized RNA duplexes were reconstituted in a 1X Universal Buffer (RNase-free and provided by Dharmacon) at a

concentration of 5 μg/μl, aliquoted, and stored at –20°C. Sequences for the duplexes used are as follows: siALK: sense 5′-AGAAGGAUGAUACGUUAUAdTdT-3′, antisense 3′-dTdTUCUUCCUACUAUGCAAUAU-5′; DsRed: sense 5′-CACCGUGAAGCUGAAGGU-GdTdT-3′, antisense 3′-dTdTGUGGCACUUCGACUUCCAC-5′.

Construction of shRNA-expressing Plasmids

SiRNA target sequences for shRNA synthesis were obtained using the Whitehead Institute for Biomedical Research's website (http://jura.wi.mit.edu/bioc/siRNA-ext/home.php). The predicted Ensembl.org chicken *Alk* sequence was entered into an analysis program which scans for sequence stretches beginning with "AA" and evaluates the thermodynamic stability of potential RNA duplexes. Negative values indicate a lower internal stability at the 5′ antisense end, suggesting a potentially more effective RNA duplex. Two siRNAs with negative thermodynamic values were selected for the construction of two hairpin vectors. One targets the sequence 5′-AAGGATGATACGTTATATATC-3′ (Alk1), and the other targets the sequence 5′-AAAGAGGATCCAATGCCGTTA-3′ (Alk2). These sequences were subjected to BLAST searches (as previously described), and no off-target genes were recognized. For the Alk1 target, DNA oligonucleotides (www.sigmagenosys.com), 5′-GGATGATACGTTATATATCTTCAAGAGAGATATATA-ACGTATCATCCTTTTTT-3′ and 5′-AATTAAAAAAGGATGATACGTTATATATCTCT-CTTGAAGATATATAACGTATCATCCGGCC-3′, were annealed and cloned into the RNA pol III expression vector, pSilencer 1.0-U6 (Ambion, Austin, TX; 7208), predigested with ApaI and EcoRI restriction endonucleases. For the Alk2 target, DNA oligonucleotides

(Sigma-Genosys) 5′-AGAGGATCCAATGCCGTTATTCAAGAGATAACGGCATTGGAT-CCTCTTTTTTT-3′ and 5′-AATTAAAAAAAGAGGATCCAATGCCGTTATCTCTTGAA-TAACGGCATTGGATCCTCTGGCC-3′ were also annealed and cloned into pSilencer 1.0-U6. The resultant constructs, pSilencerAlk1 and pSilencerAlk2, each have their oligonucleotide inserts positioned immediately after the mouse U6 promoter. Thus, the RNA product possesses sense, antisense, and intervening loop sequence allowing for short hairpin RNA formation.

In Ovo Microinjection and Electroporation

Fertilized white leghorn chicken eggs (CBT Farms, Chestertown, MD) were incubated at 37°C until Hamburger-Hamilton (HH) stage 16/17 then windowed, sealed with tape, and incubated another 24 hours before injection. Hairpin plasmids and siRNA solutions were prepared at a concentration of 2 μg/μl along with 0.1% Fast Green dye for visualization of solutions during microinjection. The GFP-producing reporter plasmid, pMES, was added to DNA/RNA solutions at 0.25 μg/μl in order to determine the efficiency of nucleic acid uptake in cells of the neural tube. This GFP plasmid also was injected alone for use as a negative control. Plasmids and siRNAs were injected into the lumen of st 22 neural tube via a drawn-out glass needle. Subsequent electroporation into half of the developing spinal cord was carried out with a BTX Electro Square Porator ECM 830 (Genetronics, Inc.) set to deliver 5 x 50 msec pulses of 24 V via a pair of gold-plated electrodes spaced 4 mm apart (Genetrodes Model 512, Genetronics, Inc.). After electroporation, several drops of 1X Hank's Balanced Salt Solution containing penicillin (100 IU/ml)/streptomycin (100 μg/ml)

(Gibco, Grand Island, NY; 15240-096) were gently placed on the embryo to cool the tissue at the site of electroporation and to prevent bacterial/mycotic contamination. Eggs were resealed with tape and returned to 37°C for 2 days until analysis at HH st 28.

Post-injection Analysis for Loss of Function

48 hours after electroporation, embryos (st 28) strongly expressing GFP were dissected and fixed in 4% paraformaldehyde in 1X PBS for 5 hours. Embryos were then processed for whole-mount in situ hybridization (without proteinase K) or embedded in OCT compound (Tissue-Tek) for cryosectioning. Following whole-mount in situ hybridization with *Alk* probe (previously described, see "In situ Hybridization"), embryos were embedded and cryosectioned. Addition of GFP antibody was necessary to restore signal in whole-mount hybridized sections since exposure to organic solvents (such as the methanol used for in situs) destroys the GFP fluorescence. In situ hybridized cryosections (40 μm) were slide-mounted, blocked with 10% NGS in TBS, pH 7.5, for 1 hour at room temperature, and incubated overnight at 4°C with mouse monoclonal anti-GFP primary antibody (Clontech, Mountain View, CA; 632375; 1:500) in 0.4% Triton X/10%NGS in TBS, pH 7.5. Slides were rinsed four times in 10% NGS and incubated for 1 hour at room temperature with a biotinylated goat anti-mouse IgG secondary antibody (Vector; BA-9200; 1:600), followed by streptavidin Alexa Fluor 568 (Molecular Probes; S-11226; 1:1000) for 2 hours, washed, and mounted in Prolong Antifade (Molecular Probes; P-7481).

Directly embedded st 28 embryos were cryosectioned (16 μm), slide-mounted and subjected to terminal deoxynucleotidyl transferase (TdT)-mediated dUTP nick end labeling

(TUNEL) assay according to the manufacturer's instructions (Roche; 12156792910) with the following changes: the concentration of sodium citrate in permeabilization solution was increased to 0.1 M, the time and temperature of slide incubation in permeabilization solution were increased to 30 minutes and 70°C respectively, incubation with TdT enzyme was increase to 4 hours, and tetramethyl rhodamine (TMR) label signal was amplified with the use of rabbit anti-TMR primary antibody (Molecular Probes; A-6397; overnight at 4°C; 1:500), followed by goat anti-rabbit IgG Alexa Fluor 568 (Molecular Probes; A-11004; 2 hours at room temperature; 1:2000). The manufacturer-recommended negative controls for the assay revealed no $TUNEL^+$ cells suggesting these changes resulted in no artificial labeling. Cryosections were also immunostained, separately from TUNEL, using anti-Isl1 (Developmental Studies Hybridoma Bank) as previously described (see "Immunohistochemistry") with a change of fluorescein avidin to streptavidin Alexa Fluor 568. Additionally, for several slides, TUNEL assay and Isl1 immunostaining were combined – nick end labeling protocols were executed first followed by co-administration of all primary and secondary antibodies utilized for both procedures with the exception that goat anti-mouse IgG Alexa Fluor 633 secondary antibody (Molecular Probes; A-21050; 1:2000) was substituted for the goat anti-mouse biotinylated antibody/streptavidin Alexa Fluor 568 used in Isl1 staining.

Images were captured using an AxioCam HRC digital video camera (Zeiss) attached to a Nikon Microphot-FXA fluorescence scope via the phototube assembly. Adobe Photoshop 7.0.1 was utilized to convert certain images to black and white, uniformly modify

image size for the photomicrographs within a figure, and adjust brightness/contrast by using the auto-levels function.

Quantitative Analysis

Three to five embryos were sectioned per experimental condition and subjected to TUNEL assay. At least 23 sections from each embryo were counted for $TUNEL^+$ cells on the electroporated and non-electroporated sides of the spinal cord. The average ratio of electroprated:non-electroporated $TUNEL^+$ cells was calculated for each embryo, and these values were used to determine the sample mean ratio and standard deviation for each condition. Sections from the thoracic region of pSilencerAlk2-injected embryos were scored in a similar fashion for $Isl1^+$ column of Terni motor neurons. To establish statistical significance, student *t*-tests were performed and *P* values calculated using the statistical software program StatDisk 10.1.0.

CHAPTER 3

RESULTS OF ALK EXPRESSION PROFILING IN CHICK

Expression of Alk mRNA in the Developing PNS

In the peripheral nervous system, prominent *Alk* expression is first detected in the cells of the sympathetic ganglia (SG) at st 19 (Fig. 1A, 1H). Inspection at later stages, including 22, 23, 24, 35, and 39, reveals the persistence of transcript in the SG with no obvious weakening of the signal intensity as far along as embryonic day 13 (E13), the latest stage investigated (Fig. 1B, 1I-1L). In the developing dorsal root ganglia (DRG), the onset of transcript becomes detectable at st 19 in the dorsal pole region (Fig. 1A, 1D). As development continues, transcript extends from the dorsal pole to the medial and lateral perimeter of the DRG and becomes more abundant with maximal expression observed at st 24/25 (Fig. 1A, 1B, 1D-F). By st 35 and beyond, *in situ* hybridization reveals no discernable *Alk* mRNA in the DRG (Fig. 1K, 1L).

In the DRG, *Alk*+ cells were localized to the dorsal pole and periphery – areas known to be composed of mitotically active cells (Rifkin et al., 2000; Wakamatsu et al., 1997). From st 22 to 27, the DRG is spatially organized with an inner core composed primarily of post-mitotic neurons surrounded by a perimeter of dividing progenitor cells (Rifkin et al., 2000). To confirm that *Alk* is expressed by mitotically active cells, *in situ* hybridization was combined with IHC to stain for the mitosis marker, H3, and traditional neuronal markers,

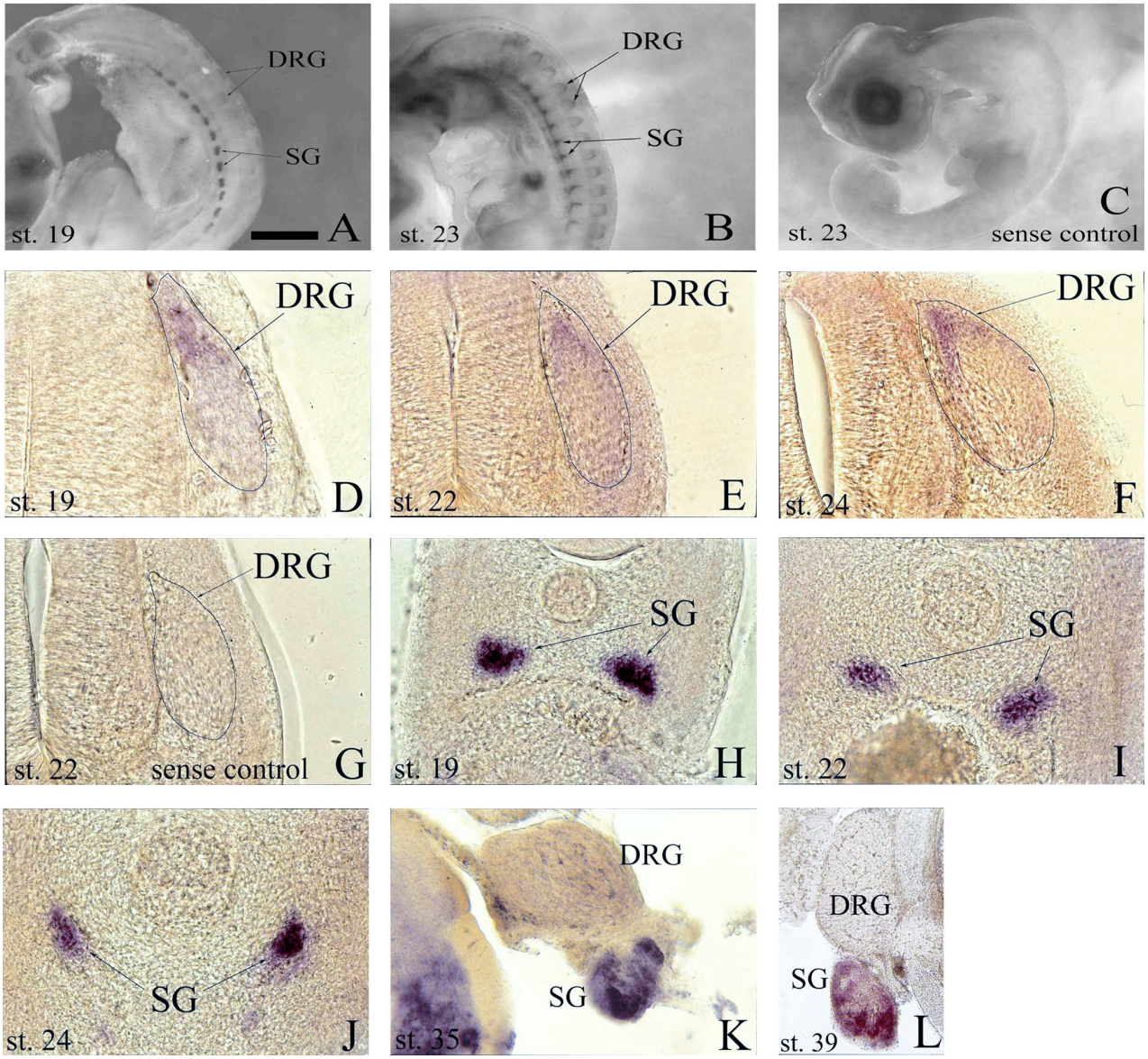


Figure 1. Analysis of developmental expression of anaplastic lymphoma kinase (*Alk*) mRNA in chick peripheral nervous system by whole-mount in situ hybridization. A,B: Transcript is expressed in both sympathetic ganglia (SG) and dorsal root ganglia (DRG) at stages 19 and 23. C: No signal is detected in stage 23 whole mounts with sense RNA probe as a negative control. D–F: Transverse sections (posthybridization) reveal *Alk* expression in the progenitor zones of the DRG at stages 19 (D), 22 (E), and 24 (F). G: Transverse section (posthybridization) of stage 22 embryo hybridized with sense RNA probe as a negative control. H–L: Transverse sections (posthybridization) show the presence of *Alk* in SG during stages 19 (H), 22 (I), 24 (J), 35 (K), and 39 (L). Scale bar: 1 mm in A (applies to A,B); 1.5 mm for C; 65 μm for D; 120 μm for E–J; 175 μm for K; 350 μm for L.

Tuj1 and Isl1. At st 23, there is no overlap of *Alk*+ and Tuj1+ cells in the DRG core nor is there apparent co-expression of Isl1 and *Alk* in this region either (Fig. 2A, 2B). In contrast, H3 staining reveals that a majority of *Alk*+ cells are located in the mitotically active dorsal pole with several H3+ cells co-expressing *Alk* (Fig. 2C). There are also *Alk*+ cells present in the progenitor zones that are neither H3+ nor Tuj1/Isl1+ suggesting that these cells are possibly preparing to enter the cell cycle, are in S-phase, or are finishing mitosis and have not yet differentiated.

In the SG, *Alk*+ cells were distributed throughout the ganglia and co-expressed markers of both mitotically active and post-mitotic cells (Fig. 2D-F). Given that the SG is unique in that dividing cells also express markers of post-mitotic neurons (Avivi and Goldstein, 1999; Rothman et al., 1978), including neurofilament (NF), Tuj1, and Isl1, the most parsimonious conclusion is that both neurons and mitotically active sympathetic precursors express *Alk*. Expression persists as late as E13 indicating that *Alk* is clearly expressed by post-mitotic neurons in both the primary and secondary chain of SG.

Expression of *Alk* mRNA in the Developing Spinal Cord

In the spinal column of chordates, MNs can be divided into two classes, those of the medial motor column (MMC) and those of the lateral motor column (LMC). The MMC is further divided into a medial portion that is present at all anterioposterior levels of the spinal cord and a lateral portion that is present only at thoracic levels. MNs of the medial MMC extend axons to axial muscles while those from the lateral MMC project axons to body wall

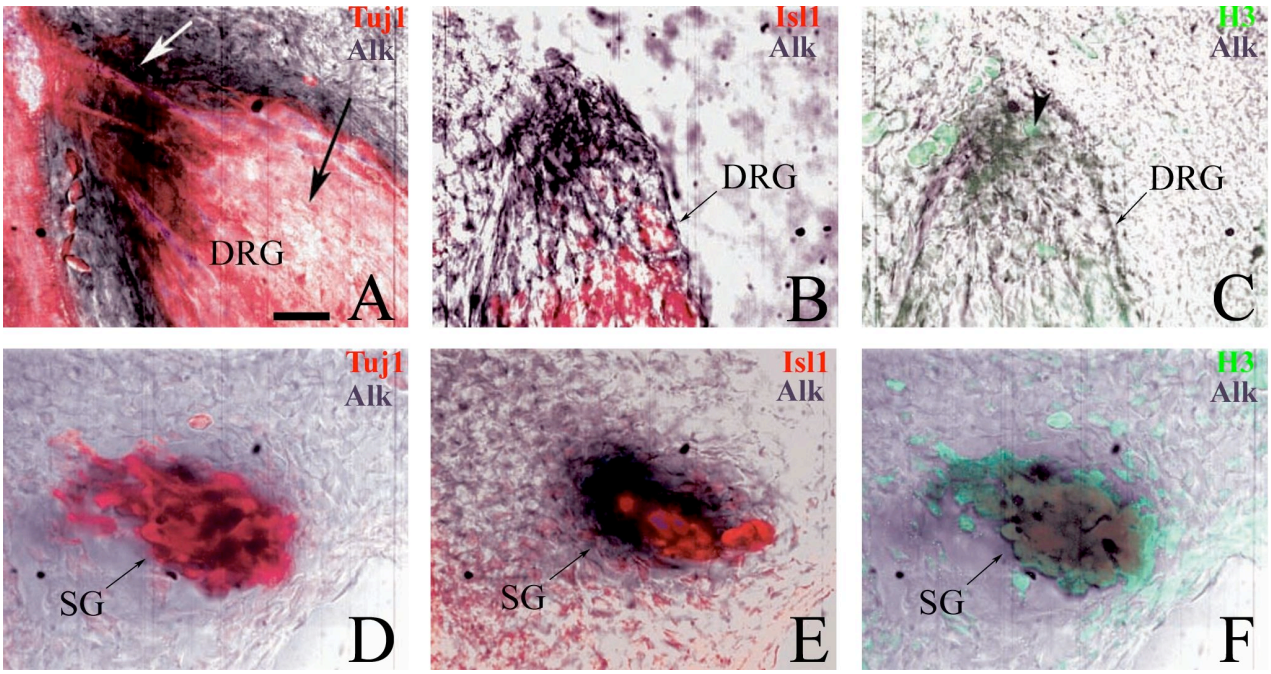


Figure 2. Anaplastic lymphoma kinase (*Alk*) mRNA is expressed in mitotically active cells of the dorsal root ganglia (DRG) and sympathetic ganglia (SG). Stage 23 embryos were vibratome-sectioned after whole-mount in situ hybridization with *Alk* probe and immunostained with α-Tuj1 or α-Isl1 and α-H3. *Alk* = dark purple, Tuj1 and Isl1 = red, H3 = green. A,B: In the DRG, *Alk* is restricted to the progenitor zone (white arrow), with no transcript present in the core (black arrow). C: Multiple cells in the dorsal pole are *Alk*+ and coexpress phosphohistone H3 (arrowhead). D–F: In the SG, most *Alk*+ cells coexpress Tuj1 (D) and H3 (F), with fewer also expressing Isl1 (E). Pseudocoloration of confocal images was performed in Adobe Photoshop 7.0.1 to depict dual signals better. Scale bar: 30 μm in A (applies to A–F).

muscles (William et al., 2003). The LMC also can be subdivided into medial and lateral subgroups, both of which are present only at limb (brachial and lumbar) levels of the spinal cord. Medial LMC MNs innervate ventrally derived limb muscles while lateral LMC MNs innervate dorsally derived limb musculature (Landmesser, 2001). To determine which divisions of MNs, if any, were expressing *Alk* during spinal cord development, transverse sections from embryos (st 24, 35 & 39) subjected to whole-mount *in situ* were collected (Fig. 3I-X) with select sections subsequently immunostained to identify MMC and LMC neurons

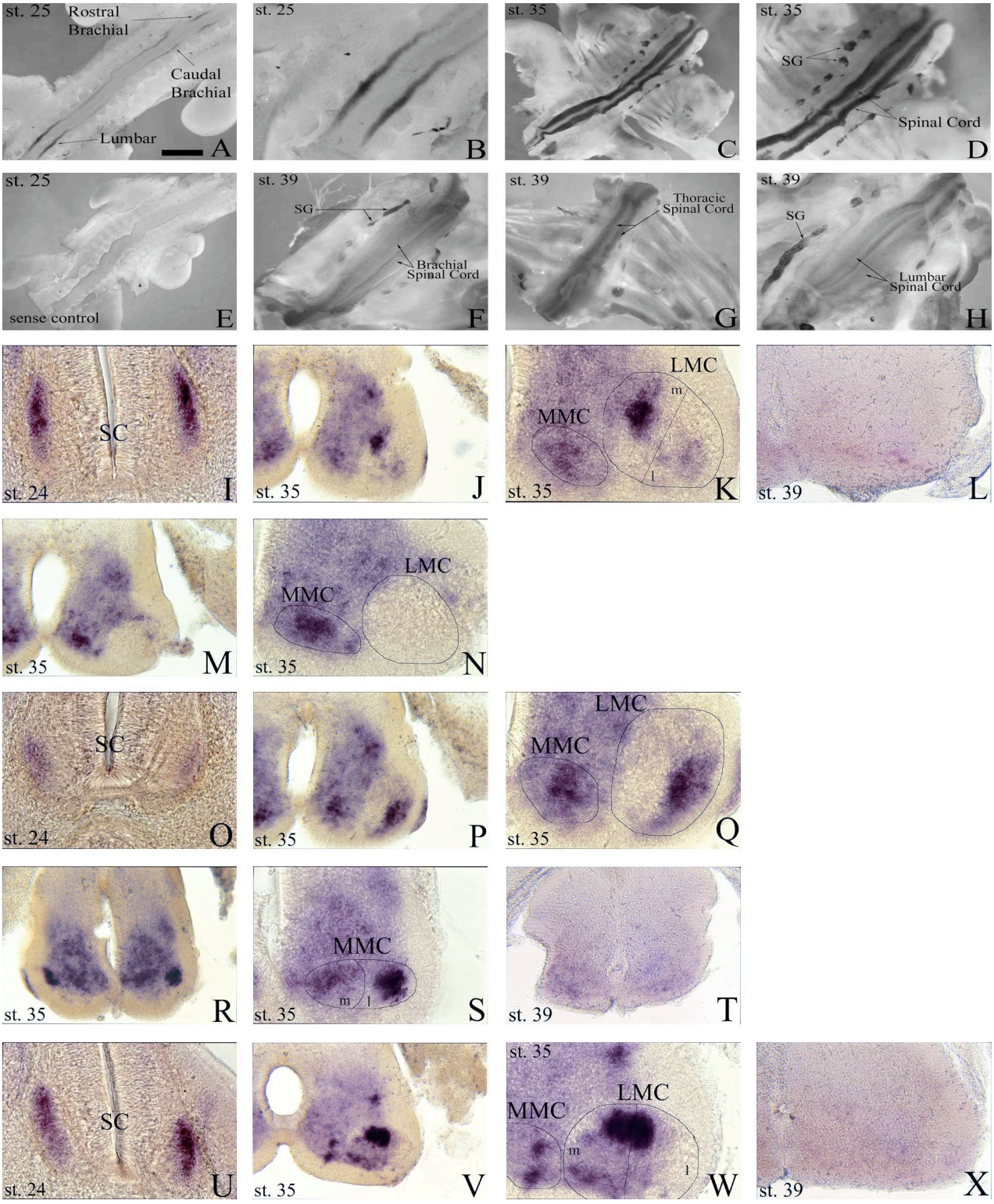

st. 25
Rostral
Brachial
Caudal
Brachial
Lumbar
A
st. 25
B
st. 35
C
st. 35
SG
Spinal Cord
D
st. 25
sense control
E
st. 39
SG
Brachial
Spinal Cord
F
st. 39
Thoracic
Spinal Cord
G
st. 39
SG
Lumbar
Spinal Cord
H
SC
st. 24
I
st. 35
J
LMC
m
MMC
l
st. 35
K
st. 39
L
st. 35
M
LMC
MMC
st. 35
N
SC
st. 24
O
st. 35
P
LMC
MMC
st. 35
Q
st. 35
R
MMC
m
l
st. 35
S
st. 39
T
SC
st. 24
U
st. 35
V
st. 35
MMC
LMC
m
l
W
st. 39
X

Figure 3. *Alk* is dynamically expressed temporally and spatially in the spinal cord. A: Transcript is restricted to brachial and lumbar regions of the spinal cord at stage 25. B: Higher magnification of lumbar region from A. C: Expression of *Alk* mRNA is detected throughout the spinal cord at stage 35. D: Higher magnification of spinal cord from C. E: No discernible expression is detected in stage 25 whole mounts with sense RNA probe as a negative control. F–H: *Alk* expression is waning in brachial (F), thoracic (G), and lumbar (H) regions of the spinal cord at stage 39. I–L: Transverse vibratome sections (posthybridization) through the rostral brachial portion of the spinal cord reveal the presence of *Alk* at stages 24 (I) and 35 (J,K), but by stage 39 (L) transcript is virtually gone. M,N: "Break" in expression where LMC is devoid of transcript, creating a rostral and caudal separation. O–Q: Vibratome sections through the caudal brachial portion of the spinal cord reveal *Alk* mRNA at stages 24 (O) and 35 (P, Q). R–T: Thoracic sections demonstrate that *Alk* is strongly expressed in spinal cord at stage 35 (R,S) but has greatly diminished by stage 39 (T). U–X: *Alk* expression in the lumbar level of the spinal cord at stages 24 (U) and 35 (V,W), with its virtual disappearance at stage 39 (X). LMC, lateral motor column; MMC, medial motor column; SC, spinal cord; SG, sympathetic ganglia. LMC and MMC were identified and demarcated based on position in the ventral portion of the spinal cord, with medial (m) and lateral (l) halves representing an estimate of where separation occurs. K, N, Q, S, and W are higher magnification views of J, M, P, R, and V respectively. Scale bar: 1 mm in A; 450 m for B; 1.7 mm for C; 1.3 mm for D,E; 1.5 mm for F–H; 100 μm for I,O,U; 160 μm for J,L,M,P,R,T,V,X; 80 μm for K,N,Q,S,W.

based on specific transcription factor (Isl1 & Lim1) expression (Fig. 4).

Nascent *Alk* expression is first detected in the chick spinal cord at st 23/24 with definitive expression occurring at st 24/25. At these early stages, transcript is restricted to the brachial and lumbar levels of the spinal cord with an interruption or "break" (devoid of transcript) within the mid-brachial region, creating a rostral and caudal component of *Alk* expression at the brachial level (Fig. 3A, 3B, 3I, 3O, 3U). Expression occurs in the lateral edge of the ventral horn corresponding to MNs of the LMC found only at limb levels (Fig. 3I, 3O, 3U). Figure 4 confirms that these *Alk*+ cells express characteristic markers of LMC MNs. At st 25, the LMC is separating into a medial and lateral half with the former's MNs expressing Isl1 and the latter's expressing Lim1 (Shirasaki and Pfaff, 2002). Immunohistochemical staining with α-Isl1 (Fig. 4B) and α-Lim1/2 (Fig. 4E) indicates that the *Alk*+ cells (Fig. 4A, 4D) are located in the prospective medial division of the LMC with the majority of them co-expressing Isl1 (Fig. 4C, 4F).

At st 35, expression is no longer restricted to limb regions, and *Alk* mRNA is detected

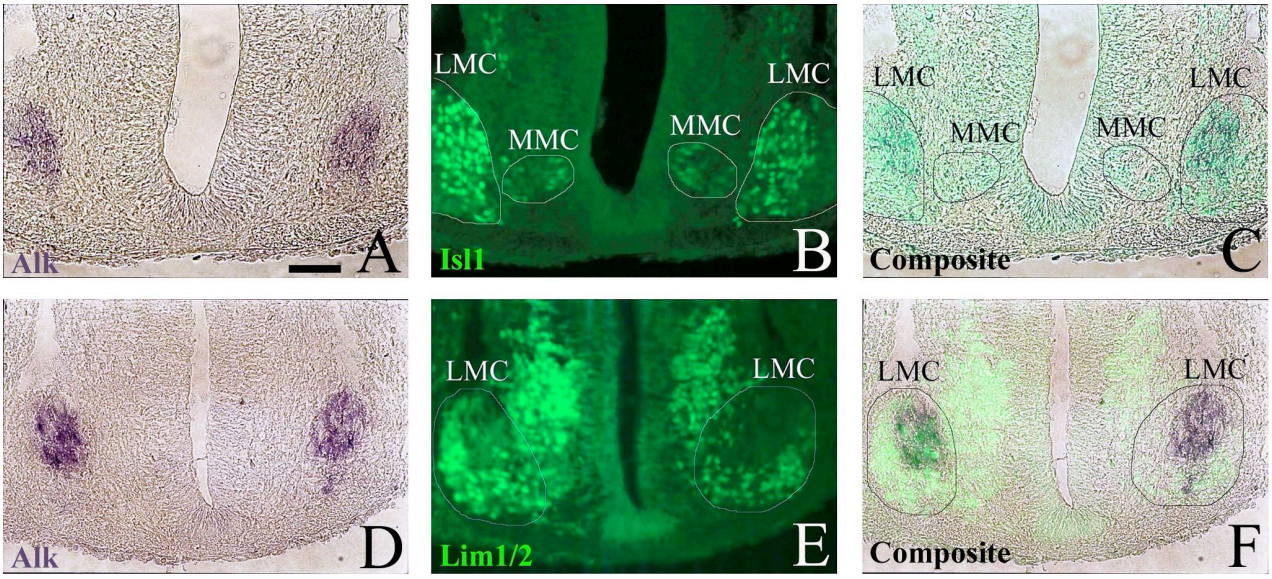


Figure 4. *Alk* is expressed by discrete subpopulations of motor neurons. A,B: Stage 25 embryo from *Alk* whole-mount in situ hybridization (dark purple) was cryosectioned and then immunostained for Isl1 (green). C: *Alk* and Isl1 staining are shown overlaid as a composite. D,E: Stage 25 embryo from *Alk* whole-mount in situ hybridization (dark purple) was cryosectioned and then immunostained for Lim1/2 (green). F: *Alk* and Lim1/2 staining are shown overlaid as a composite. Medial motor column (MMC) and lateral motor column (LMC) have been demarcated. The MMC and medial half of the LMC are known to express Isl1; however, the lateral half of the LMC does not. Conversely, the lateral LMC expresses Lim1, whereas the MMC and medial LMC do not. Positional identification of *Alk* and motor column markers indicates that *Alk* is limited to cells of the LMC. Composite images were created in Adobe Photoshop 7.0.1. Scale bar: 50 μm in A (applies to A–F).

in MMC neurons at every level of the spinal cord (Fig. 3C, 3D, 3J, 3K, 3M, 3N, 3P-S, 3V, 3W) with the lateral MMC staining strongly at thoracic levels (Fig. 3S). It is worth mentioning that while *Alk* expression was not investigated thoroughly in cervical and sacral regions, *Alk* transcript throughout the MMC at these levels was diffusely and uniformly expressed (data not shown). Additionally, *Alk* is expressed by LMC MNs at brachial and lumbar levels, and the "break" in expression, seen in the st 24/25 brachial region, still remains (Fig. 3K, 3N, 3Q, 3W). There are also additional areas where transcript is expressed more uniformly in the spinal cord dorsal to the MMC and LMC (Fig. 3J, 3P, 3V). Based on their location, it is likely that dorsal interneurons and possibly V2 or V1 interneurons are

expressing *Alk*, but further identification using specific interneuron markers would be needed for confirmation. By stage 39, transcript signal diminishes throughout the spinal cord with expression in the brachial and lumbar regions virtually non-existent (Fig. 3F-3H, 3L, 3T, 3X). Figure 5 summarizes the spatial-temporal expression of *Alk* in the embryonic spinal cord, sympathetic ganglia, and dorsal root ganglia.

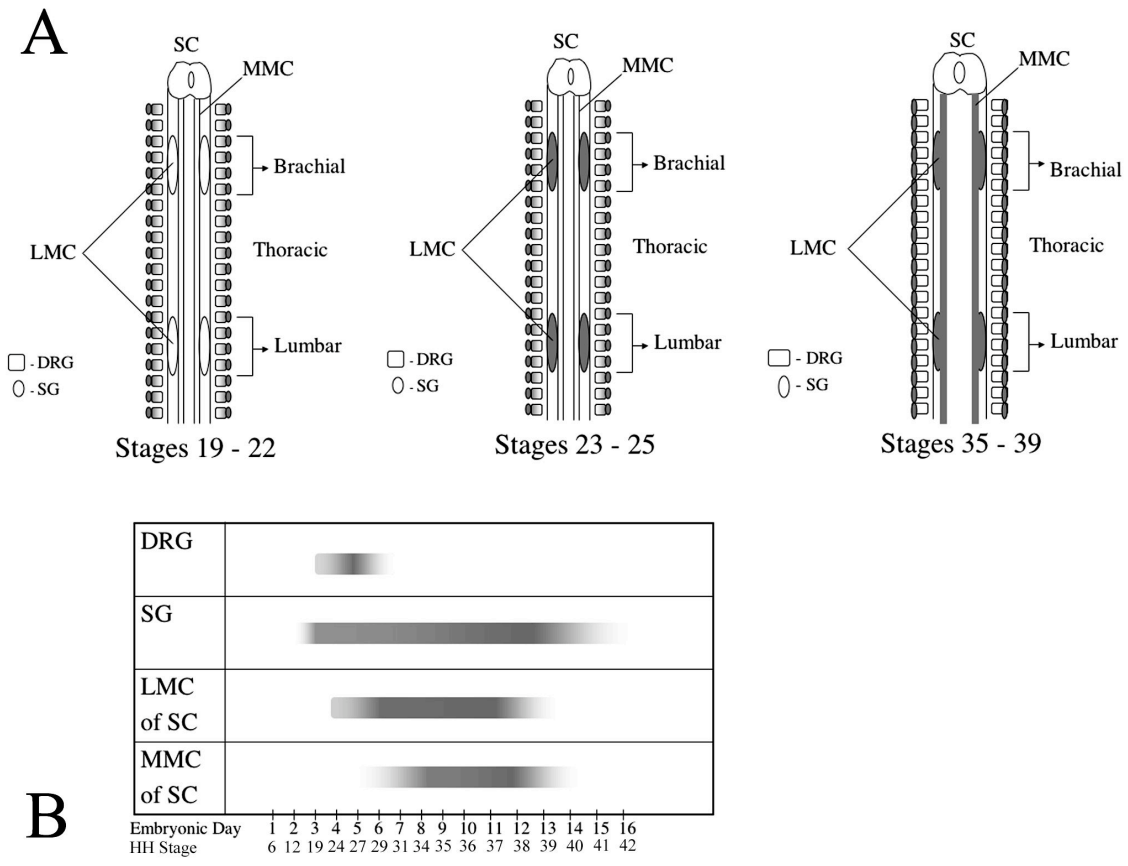


Figure 5. Spatial-temporal overview of anaplastic lymphoma kinase (*Alk*) mRNA expression in developing chick nervous system. A: Spatial schematic of *Alk* expression (shading) with emphasis on location of transcript during investigated time points. B: Temporal schematic of *Alk* expression (bars), with emphasis on span of transcript duration in the embryonic PNS and spinal cord. Solid bar ends denote the definitive identification of a start point regarding *Alk* expression. Diffuse bar ends denote that a definitive start or end point was not identified from the time points analyzed in this investigation. Depth of shading within the bars is a reflection of the intensity of *Alk* expression. SC, spinal cord; MMC, medial motor column; LMC, lateral motor column; DRG, dorsal root ganglia; SG, sympathetic ganglia.

Alk Expression in Hind Limb and Body Wall Musculature

In the course of whole-mount *in situ* hybridization, *Alk* expression was detected in st 35 hind limb and body wall muscles. Within the musculature of the thigh and shank, *Alk* transcript is present in the iliotibialis cranialis (Fig. 6A), iliotibialis lateralis (Fig. 6B), caudofemoralis (Fig. 6C), fibularis longus (Fig. 6D), and gastrocnemius externus (Fig. 6D); identification of hind limb muscles based on findings of Kardon (1998). Expression was also observed in the intercostals of the body wall (Fig. 6E). It is of interest to note that the intercostals are the target muscles that are innervated by MNs from the lateral MMC which also expresses *Alk* mRNA (Fig. 3S); Sharma et al. (2000). Whether or not the aforementioned thigh and shank muscles are targets innervated by *Alk*+ MNs of the lumbar LMC remains to be determined.

Limb-derived Cues and the Regulation of *Alk*

The onset of *Alk* expression in the spinal cord (st 23/24) overlaps temporally with the expression of ETS family genes. Lin et al. (1998) demonstrated that ETS transcription factors are potentially involved in the development of selective sensory-motor circuits in the spinal cord and that signals from the limb control the expression of *Ets* genes. Because of the temporal coincidence of *Alk* and *Ets* gene expression, we were curious if *Alk* was also regulated by limb-derived cues and if ALK or ETS factors might regulate the expression of each other. To test this, we ablated one hind limb from embryos at st 17/18 and allowed

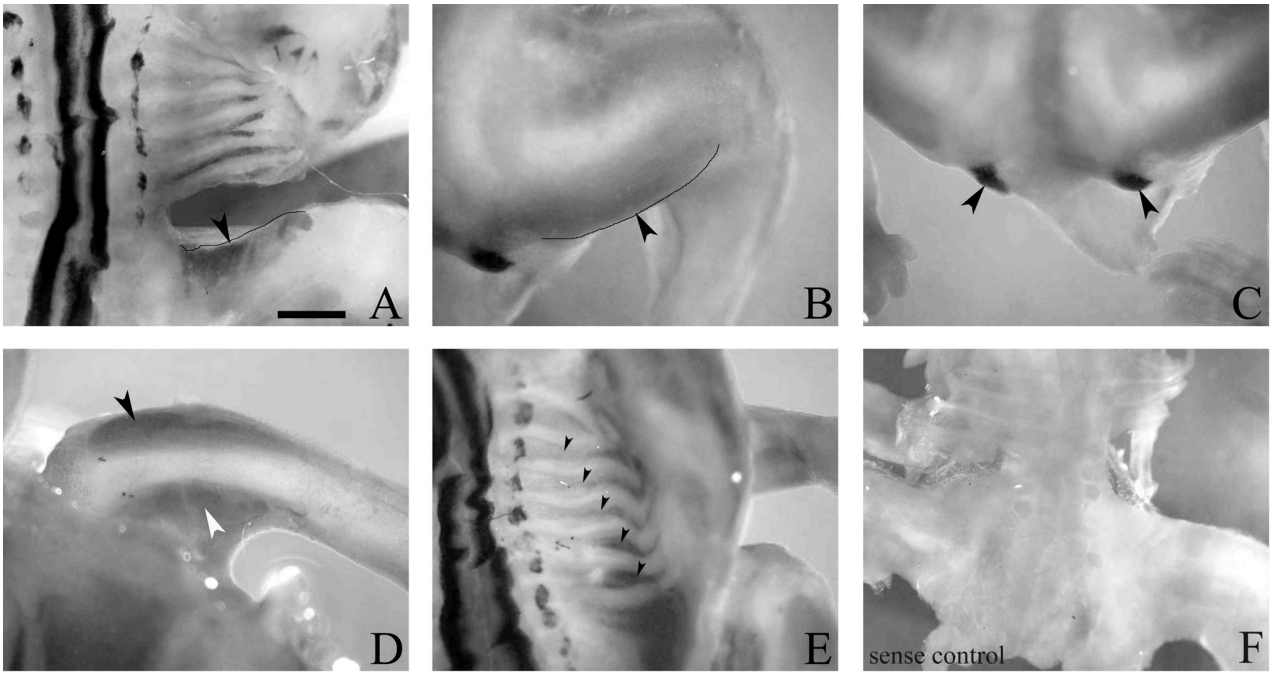


Figure 6. *Alk* is expressed by subsets of hind limb and body wall muscles. Stage 35 whole-mount in situ hybridization reveals *Alk* mRNA in the iliotibialis cranialis (A; arrowhead), iliotibialis lateralis (B; arrowhead), caudofemoralis (C; arrowheads), fibularis longus (D; black arrowhead), gastrocnemius externus (white arrowhead), and intercostals (E; arrowheads). F: No transcript was detected in stage 35 whole-mount with sense RNA probe as a negative control. Scale bar: 1 mm in A (applies to A–C,E); 750 μm for D; 1.3 mm for F.

to develop until st 23/24. The embryos were then hybridized with *Alk* antisense probe to determine whether limb cues were required for *Alk* expression. Unlike *Ets* genes, *Alk* mRNA is still present in the CNS and PNS at levels comparable to the control (intact) side of ablated embryos after limb removal (data not shown). These results provide evidence that *Alk* expression is not under the control of signals produced by the limb. Based on these data, it is also unlikely that there is an influence on *Ets* gene expression by ALK or vice versa.

CHAPTER 4

RESULTS OF ALK KNOCKDOWN IN CHICK SPINAL CORD

Targeted Silencing of Anaplastic Lymphoma Kinase in Chick Spinal Cord

Based on the results from *Alk* expression profiling, it was decided that functional analysis of *Alk* in vivo would focus on the receptor's role in spinal cord development. We constructed plasmids expressing short hairpin RNAs (pSilencerAlk1 and pSilencerAlk2), each targeting a distinctly different sequence of chicken *Alk* (Fig. 7). Additionally, a commercially synthesized siRNA duplex (siALK) was obtained in order to knockdown endogenous levels of *Alk* expression. Thus two separate RNAi methodologies were employed to assess the effects of *Alk* gene silencing in chick.

Using parallel sets of embryos, each of the three treatments was injected separately into the lumen of st 22 neural tube and electroporated (Fig. 8) – a plasmid expressing GFP (pMES) was also co-injected in order to identify the electroporated hemisphere and to determine electroporation efficiency. To evaluate whether observed *Alk* silencing was target specific or a result of any siRNA or simply a consequence of electroporation with nucleic acid, another set of embryos were electroporated with siRNA targeting the non-endogenous fluorescent reporter DsRed or with pMES only.

Both pSilencerAlk1 and pSilencerAlk2, as well as siALK, reduced expression of *Alk* transcript in the electroporated half of st 28 spinal cord (determined by in situ hybridization for *Alk*) with pSilencerAlk2 yielding the lowest apparent mRNA levels (Fig. 9A, B, D-G).

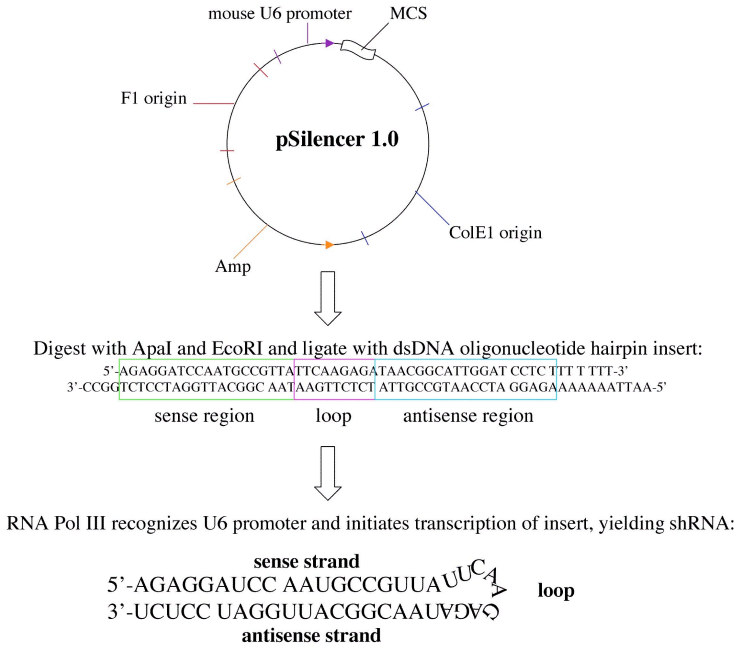


Figure 7. Schematic representation of shRNA plasmid construction. Template DNA, containing sense, loop, and antisense sequence, was inserted into Ambion's pSilencer1.0-U6 vector. Subsequent transcription via the U6 promoter and RNA Polymerase III yields RNA capable of hairpin and duplex formation. MCS, multiple cloning site; Amp, ampicillin resistance.

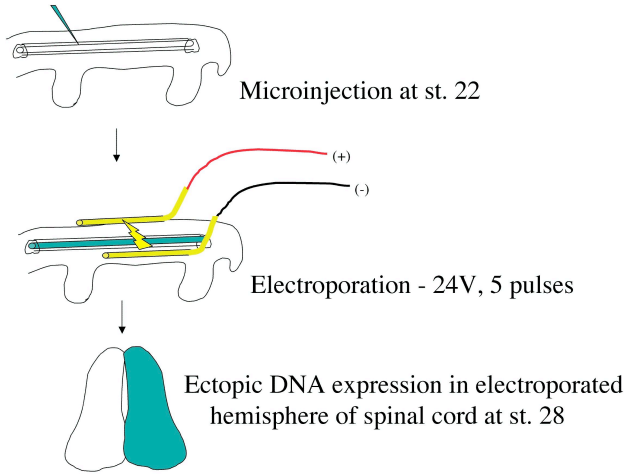


Figure 8. Cartoon diagram of microinjection and electroporation of nucleic acid in chick neural tube at st 22. A drawn-out glass needle was used to inject plasmid DNA or siRNA solution (teal) into the lumen of the tube. Five pulses of 24V were administered with the use of gold-plated electrodes in order to drive the nucleic acid of choice into cells of the neural tube. Two days later at st 28, cells of the electroporated hemisphere were inspected for reduced transcript levels and any phenotypic changes as compared to the control or non-electroporated side.

However, levels of *Alk* expression remained unchanged after transfection with either pMES vector alone (Fig. 9C) or DsRed siRNA (Fig. 9H). These data demonstrate that effective, target-specific knockdown of *Alk* transcript was achieved.

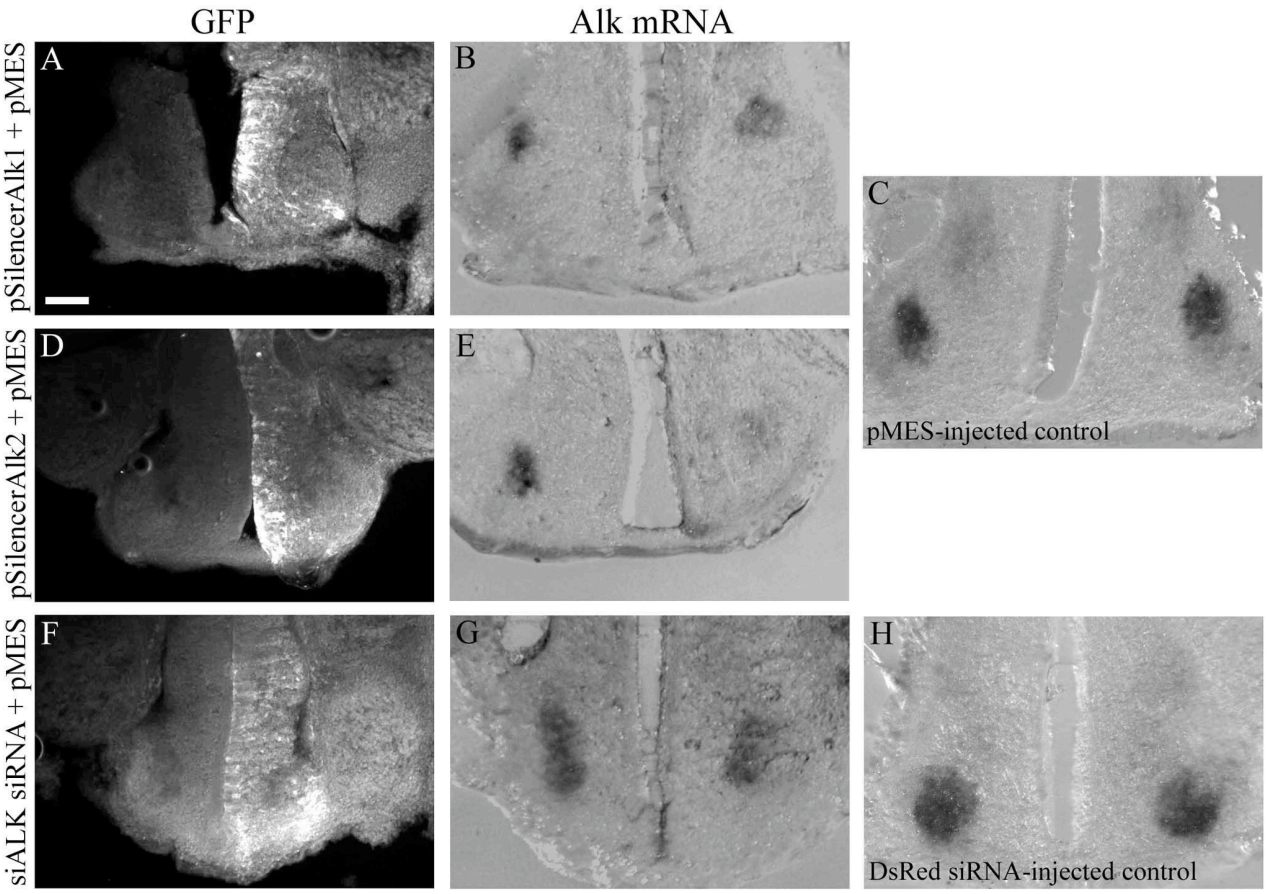
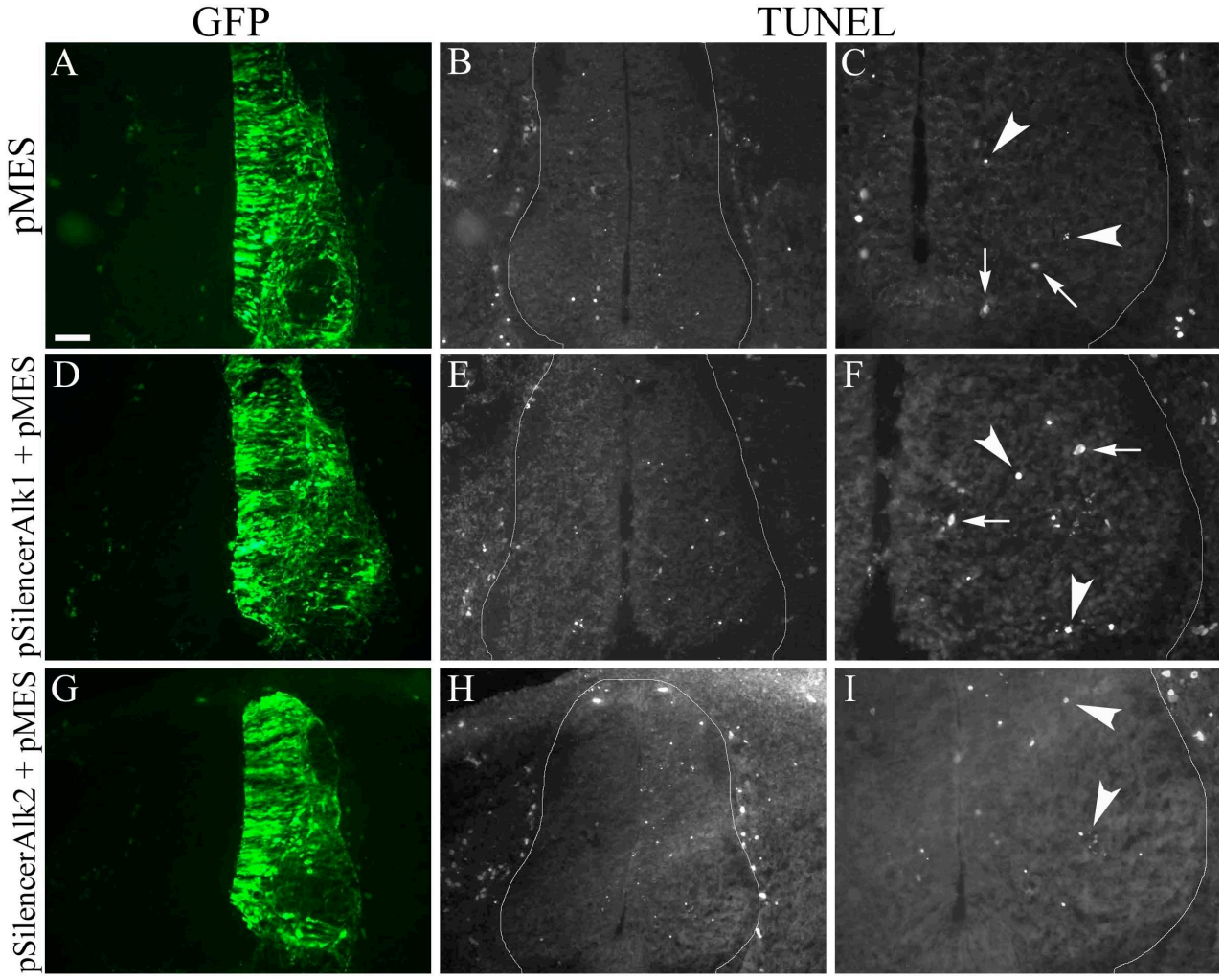


Figure 9. Knockdown of *Alk* transcript in spinal cord is target-specific. Right side of the spinal cord is electroporated as indicated by expression of GFP (A, D, F). *Alk* mRNA expression after electroporation of pSilencerAlk1 (A, B), pSilencerAlk2 (D, E), and siALK siRNA (F, G) in st 28 embryos. Each treatment results in decreased levels of *Alk* mRNA on the electroporated side. Embryos electroporated with pMES only (C) or DsRed siRNA (H) show no loss of *Alk* transcript in electroporated side (right) versus non-electroporated side (left). Scale bar = 130 μm in A (applies to A, D, F); 95 μm for B, C, E, G, H.

Increased Cell Death in Developing Spinal Cord after *Alk* Knockdown

In the chick spinal cord, programmed cell death (PCD) of motor neurons begins at approximately st 26/27 and ends at roughly st 38 (Gould and Oppenheim, 2004; Okado and Oppenheim, 1984). Because Alk is prominently expressed in motor neurons during the entire period of PCD, an analysis of how *Alk* gene silencing impacts cell death seemed warranted.

To establish that electroporation and/or the introduction of foreign DNA/RNA into cells was not generating a non-specific cytotoxic effect, control pMES-injected and DsRed-injected embryos were cryosectioned and assayed for cell death by means of terminal deoxynucleotidyl transferase-mediated dUTP nick end labeling (TUNEL) (Fig. 10A-C and Fig. 11A-C). The number of dead cells was roughly equal in both hemispheres of the spinal cord resulting in a ratio of electroporated TUNEL+ cells:non-electroporated TUNEL+ cells approximately equal to 1 for both sets of embryos (Fig. 10J and Fig. 11G). More than likely, this suggests that no cytotoxicity was caused by electroporation of any nucleic acid since one would expect a roughly equal number of apoptotic cells in both halves of a normally developing spinal cord. However, when embryos electroporated with pSilencerAlk1, pSilencerAlk2, or siALK (all co-electroporated with pMES) were cryosectioned and subjected to TUNEL staining, increased cell death was observed on the electroporated side in comparison to the non-electroporated side (Fig. 10D-I and Fig. 11D-F). Normalized against negative controls, ratios of electroporated:non-electroporated TUNEL+ cells revealed a 1.3-fold, 2-fold, and 2.7-fold increase in cell death on the electroporated side for embryos treated


GFP
TUNEL
A
B
C
pMES
D
E
F
pSilencerAlk1 + pMES
G
H
I
pSilencerAlk2 + pMES

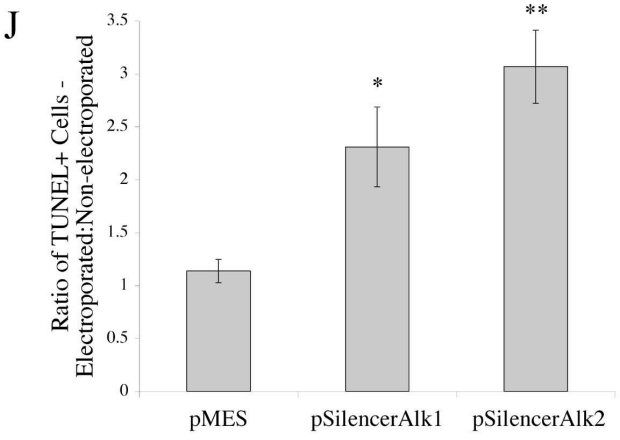

J
Ratio of TUNEL+ Cells - Electroporated:Non-electroporated
3.5
3
2.5
2
1.5
1
0.5
0
*
**
pMES
pSilencerAlk1
pSilencerAlk2

Figure 10. *Alk*-specific hairpin constructs lead to increased cell death in chick spinal cord. A-C: Transverse cryosection from st 28 pMES only-injected embryo expressing GFP on electroporated side (A) and stained for TUNEL (B, C). C is a higher magnification of electroporated side in B. D-F: Transverse cryosection from st 28 pSilencerAlk1-injected embryo expressing GFP on electroporated side (D) and stained for TUNEL (E, F). F is a higher magnification of electroporated side in E. G-I: Transverse cryosection from pSilencerAlk2-injected embryo expressing GFP on electroporated side (G) and stained for TUNEL (H, I). I is a higher magnification of electroporated side in H. J: Ratios of electroporated:non-electroporated TUNEL+ cells (mean ± std. dev.) for pMES-treated (n = 3), pSilencerAlk1-treated (n = 5), and pSilencerAlk2-treated (n = 5) embryos (* $P = 0.0011$; ** $P < 0.0001$). Arrowheads denote examples of nuclei with intense fluorescence and morphologies characteristic of apoptotic bodies that were counted, whereas larger, more diffusely staining artifacts (arrows) were not. Scale bar = 100 μm in A (applies to A, B, D, E, G, H); 50 μm for C, F, I.

with siALK, pSilencerAlk1, and pSilencerAlk2 respectively (Fig. 10J and Fig. 11G). Cell death in the control-injected embryos was limited primarily to the ventral portion of the cord (Fig. 10B and Fig. 11B). With silencing treatments, cell death was observed in areas where *Alk* is known to be expressed, meaning both ventral and dorsal regions of the cord exhibited increased cell death when compared to controls (Fig. 10E, H and Fig. 11E). However, there was no formal distinction with regard to subcategorizing dorsal versus ventral TUNEL+ cells because any meaningful separation and classification would require a combinatorial approach of TUNEL and immunostaining for interneuron and motor neuron populations in order to accurately identify the subtype of dying cells.

Identification of Phenotypic Changes in Specific Neuronal Populations

To identify with greater certainty increased cell death in specific neurons that corresponded topographically to motor neurons, we observed cell populations expressing the molecular marker Isl1 for phenotypic changes upon *Alk* knockdown. Isl1 immunostaining identifies motor neurons from the LMC, MMC, and column of Terni (CT) (Shirasaki and Pfaff, 2002; William et al., 2003). Because Isl1+ cells were too numerous and densely layered for accurate counting in the LMC and MMC, a more direct approach of combined

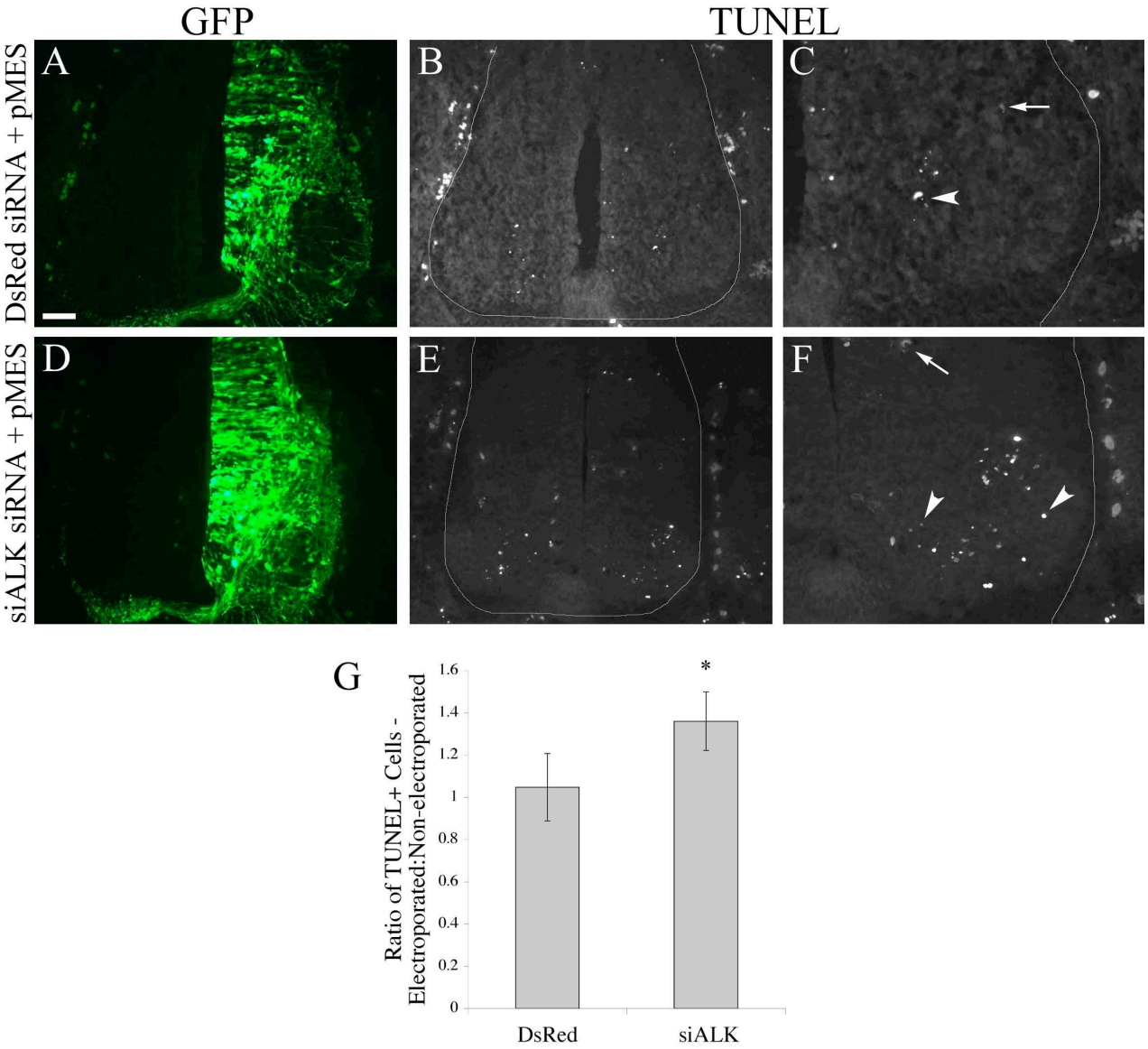


Figure 11. Pre-synthesized *Alk*-specific siRNA leads to increased cell death in chick spinal cord. A-C: Transverse cryosection from st 28 DsRed-injected embryo expressing GFP on electroporated side (A) and stained for TUNEL (B, C). C is a higher magnification of electroporated side in B. D-F: Transverse cryosection from st 28 siALK-injected embryo expressing GFP on electroporated side (D) and stained for TUNEL (E, F). F is a higher magnification of electroporated side in E. G: Ratios of electroporated:non-electroporated TUNEL+ cells (mean ± std. dev.) for DsRed-treated (n = 3) and siALK-treated (n = 4) embryos (* $P < 0.02$). Arrowheads denote examples of nuclei with intense fluorescence and morphologies characteristic of apoptotic bodies that were counted, whereas larger, more diffusely staining artifacts (arrows) were not. Scale bar = 100 μm in A (applies to A, B, D, E); 50 μm for C, F.

TUNEL and Isl1 staining was used to identify regions where increased cell death was observed after *Alk* silencing.

Co-staining revealed that increased cell death in the electroporated side of ventral cord occurs in LMC and MMC motor neurons (Fig. 12). Additional Isl1 staining in the thoracic region identified a significant decrease in the number of Isl1+ CT motor neurons, topographically overlapping with the same region exhibiting increased cell death in TUNEL-stained thoracic sections from the same embryos (data not shown), in pSilencerAlk2-electroporated embryos when compared to pMES only-electroporated embryos (Fig. 13). Because no expansion of Isl1+ cells into foreign areas was observed and *Alk* is not expressed in CT motor neuron progenitors as they leave the ventricular zone to mature (st 24), the decrease is not likely attributable to an influence of *Alk* on columnar organization/cell migration or motor neuron differentiation. The approximately 60% decrease in CT cells on the electroporated side (Fig. 13E-G) suggests that sympathetic preganglionic motor neurons are likely among the more dorsal-medially located cells experiencing premature death in thoracic spinal cord of pSilencerAlk2-treated embryos.

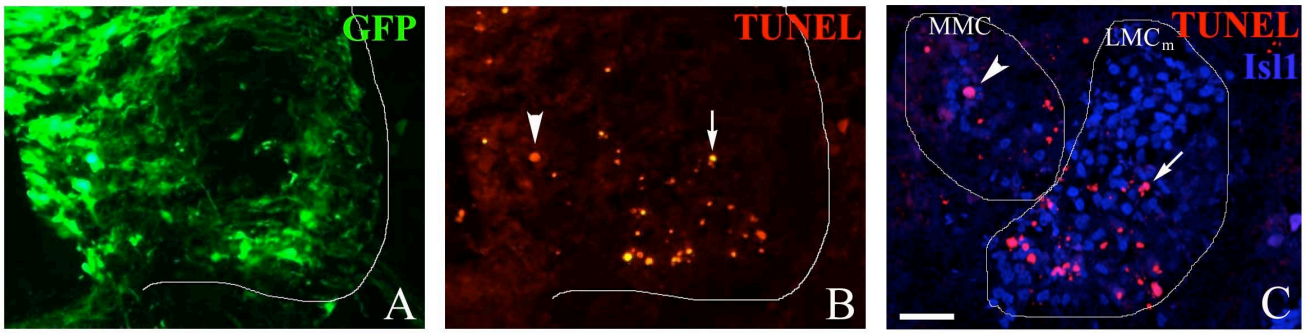


Figure 12. *Alk* silencing induces premature cell death in somatic motor neurons. A-C: Transverse cryosection from st 28 pSilencerAlk1-injected embryo expressing GFP on electroporated side (A) and stained for TUNEL (B) and Isl1 (C). TUNEL+ cells are localized within medial and lateral motor columns with several dying cells still expressing Isl1 (pink nuclei). Arrowheads and arrows are reference markers identifying the same nuclei in B and C. MMC, medial motor column; LMC_m, medial portion of the lateral motor column. Scale bar = 60 μm for A and B; 30 μm for C.

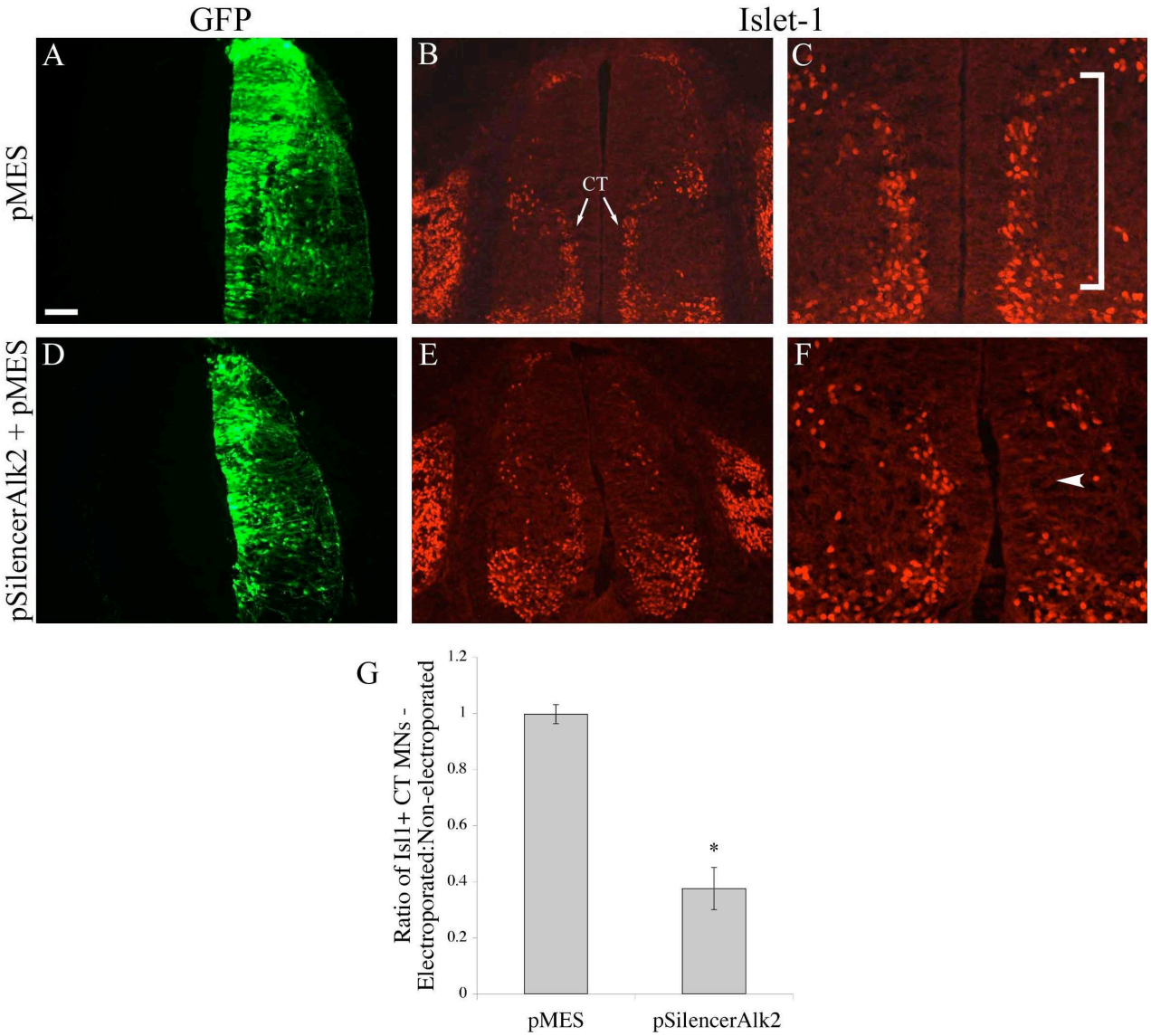


Figure 13. Isl1+ thoracic column of Terni motor neurons fail to survive after *Alk* knockdown. A-C: Transverse cryosection from st 28 pMES-injected embryo expressing GFP on electroporated side (A) and stained for Isl1 (B, C). C is a higher magnification of columns in B; the bracket encompasses the area occupied by preganglionic motor neurons. D-F: Transverse cryosection from st 28 pSilencerAlk2-injected embryo expressing GFP on electroporated side (D) and stained for Isl1 (E, F). F is a higher magnification of columns in E; arrowhead denotes the conspicuous lack of Isl1+ neurons on the electroporated side. G: Ratios of electroporated:non-electroporated Isl1+ cells (mean ± std. dev.) for pMES-treated (n = 2) and pSilencerAlk2-treated (n = 3) embryos (* $P = 0.0009$). CT, column of Terni. Scale bar = 100 μm in A (applies to A, B, D, E); 50 μm for C, F.

CHAPTER 5

DISCUSSION

Pertaining to the initial phase of this thesis work, the first in-depth characterization of *Alk* expression in the developing spinal cord and peripheral nervous system is reported. This analysis identified three CNS and PNS neural structures which express *Alk* in a temporally dynamic pattern that correlates with key developmental events in each neural component. Given the ease of conducting gain and loss of function experiments in the chick, this expression profile provides the necessary foundation for determining ALK's function during development of MNs, SG, and DRG *in vivo*.

Alk Expression in the Sympathetic Ganglia is Robust and Temporally Extensive

First detected at st 19 (~E3), *Alk* in the SG has an intense and sustained expression lasting at least through st 39 (E13), the latest time-point examined. Thus the course of *Alk* expression in the SG encompasses the periods of proliferation, differentiation, and PCD in addition to the formation of both the primary and secondary chain of sympathetic ganglia. According to Rothman et al. (1978), proliferation takes place from E2-3 to E21 with fewer and fewer cells dividing as time progresses. Our findings show that at E4 a majority of *Alk*+ cells are mitotically active, co-expressing phosphohistone H3. Because traditional differentiation markers like Tuj1 and Isl1 can be expressed in cells that are still mitotically active in the SG, attempts to identify differentiated, post-mitotic *Alk*+ neurons in st 23 SG proved to be ambiguous. However, it has been determined that virtually all SG neurons have

exited the cell cycle between E8 and E12 (Smet et al., 1986). Additionally, pyknotic neurons are found throughout development, but cell death is most prominent from E7 to E18 (Smet et al., 1986). Since *Alk* mRNA is transcribed during these developmentally significant times, ALK most likely participates in the genesis, maturation, and/or survival of sympathetic neurons. Thus, elucidating ALK's function during SG development will expand our understanding of the extracellular signals that regulate SG development which heretofore have focused primarily on the neurotrophins.

Restricted Expression of Alk in the DRG to Mitotically Active Progenitors

Hamburger et al. (1981) identified a region of small, immature cells that are mitotically active in the medial and dorsolateral perimeters of the DRG, from which, he proposed, the second wave of neurons is derived. These peripheral zones of proliferating progenitors are separate from the core that contains the first wave of early-differentiating post-mitotic neurons. Results from this study show that *Alk* expression is confined to the proliferative margins (rather than the interior neural core) from st 19 to 25 and is non-detectable by st 35. Within the progenitor zones, there are mitotically active *Alk*+ cells in addition to *Alk*+ cells that are neither dividing nor differentiated. These data suggest that ALK may be involved in regulating the proliferation of progenitor cells or their exit from the cell cycle in preparation for differentiation. In addition or alternatively, *Alk* might promote the survival of DRG progenitor cells. Since *Alk* is not expressed in the inner neural core of the DRG nor is it expressed during the period of PCD of post-mitotic neurons (Carr and Simpson, 1978; Hamburger et al., 1981), ALK is not a candidate receptor for mediating

function in post-mitotic neurons. Thus, this is the first RTK identified to be expressed exclusively in DRG progenitor cells. Given our lack of understanding of the signals that regulate the mitogenesis, differentiation, or survival of DRG progenitor cells, further investigation of ALK's function in the DRG will be insightful.

Alk mRNA is Differentially Expressed in Motor Neuron Subsets and in Muscle Subsets of the Hind Limb and Body Wall

This study demonstrates that *Alk* is expressed by discrete subpopulations of MNs. Collectives of *Alk*-expressing MNs are confined to the MMC and LMC of the developing spinal cord; although, *Alk* is first detected in only the LMC at st 23/24 with expression in the MMC following later in development. This temporal difference in expression is possibly explained by the differing birthdates of MNs in the LMC and MMC. The majority of brachial and lumbar LMC are born by st 22, whereas most of the MMC neurons are generated by st 24 (Hollyday and Hamburger, 1977; Prasad and Hollyday, 1991). Due to this time lag between the genesis of LMC and MMC MNs, a corresponding lag in the onset of *Alk* expression between these two groups would be expected.

Sectioning through E8.5-9 spinal cord at various axial levels reveals specific clusters of *Alk*+ cells within the LMC and MMC that change position upon progression through a particular column. Each spatial cluster, known as a motor pool, is a subdivision of MNs that collectively innervate a specific muscle (Hollyday, 1980; Landmesser, 1978). While several muscles, including the iliotibialis cranialis, iliotibialis lateralis, caudofemoralis, fibularis longus, and gastrocnemius externus, also expressed *Alk*, further study will be required to

determine if they are innervated by the lumbar motor pools that also express *Alk*. In the thorax, MNs from the lateral half of the MMC in addition to their target musculature, the intercostals, both express *Alk* mRNA. Thus, ALK could participate in a matching mechanism to insure correct target innervation. One such mechanism could involve the guidance of axons and myotubes, via ALK and interactions with its ligand, to a common point where nerve and target are proximally "matched."

Additionally, *Alk* expression in MNs overlaps temporally with the period of PCD from E5-E12, peaking at E8 (Okado and Oppenheim, 1984; Gould and Oppenheim, 2004). Furthermore, *Alk* expression coincides temporally with the establishment of columnar organization, but not columnar identity which has been determined prior to *Alk* expression (Okado and Oppenheim, 1984; Sockanathan et al., 2003; Tsuchida et al., 1994). It is also worth noting that *Alk* is expressed during the period of synapse formation (st 28-36) (Fredette and Ranscht, 1994). Therefore, if ALK is involved in synaptogenesis, it most likely does not have the role of destabilizing or inhibiting synapse differentiation, as is proposed by Liao et al. (2004) in *C. elegans*, since one would then anticipate a reduction in mRNA expression over this time period so that synapse stabilization could occur.

PCD in spinal motor neurons is profound, leading to the elimination of 50% of the MNs that are generated (Oppenheim, 1991). It is clear from the rich body of literature on MN cell death that not all MN survival can be mediated by currently identified neurotrophic factors. Thus, there may be as yet unidentified ligand/receptor interactions that regulate MN survival.

Because of its noticeable transcript expression in MNs during the peak of PCD, the second phase of investigation focused on ALK's in vivo role regarding spinal cord development – specifically, its involvement in neuronal survival. Through use of RNA interference, *Alk* gene silencing was achieved in chick spinal cord. Subsequent analyses revealed that *Alk* knockdown leads to increased cell death with somatic and visceral motor neurons among the targeted cells.

Similar Phenotypic Changes Observed with Use of Different RNAi Methodologies

These studies utilized two separate method of RNAi, in ovo electroporation of shRNA plasmid and electroporation of chemically synthesized siRNA, in an attempt to corroborate, by different means, any observed phenotypic changes. In addition, an added level of validation was achieved with injection and electroporation of two different shRNA plasmids, targeting separate sequence sites of chicken *Alk*. All three treatments, the siRNA and two hairpin constructs, resulted in a target-specific decrease of *Alk* transcript, leading to increased cell death in areas of chick spinal cord known to express *Alk*.

While all yielded similar general changes, there were varying degrees of effectiveness among the treatments. For example, shRNA plasmids seemed more potent silencers of *Alk* since lower levels of transcript and more cell death were observed than with siALK siRNA. This phenomenon may be attributable to the fact that pre-synthesized siRNA is introduced into cells as a concentrated bolus, and over time the limited supply of RNA duplexes are processed and broken down without replacement. It is plausible that two days after electroporation, their quantity and, thusly, potency has begun to diminish. Short hairpin

RNAs, however, are continually expressed from plasmids so their quantity is not as limited and knockdown is sustained. Even between the two shRNAs there appears to be greater efficacy of pSilencerAlk2 over pSilencerAlk1. In this instance, pSilencerAlk2 may have sequence characteristics that yield more effective shRNAs, or the electroporation efficiency may have been slightly greater for pSilencerAlk2-treated embryos, transfecting more cells than in embryos electroporated with pSilencerAlk1. Despite differences in treatment potency, these data demonstrate a similarly reproduced increase in cell death using two different RNA interference tactics.

ALK Promotes Cell Survival of Somatic and Visceral Motor Neurons

Our loss-of-function analyses reveal that premature cell death occurs within specific populations of motor neurons where the presence of *Alk* mRNA has been characterized. Motor neurons from the LMC, MMC, and thoracic CT were identified and demonstrated conspicuous signs of increased premature cell death caused by *Alk* silencing. Hence, these data suggest that ALK influences the survival of both somatic and visceral motor neurons, although the degree of impact may differ between the two.

All neurotrophins (except nerve growth factor), chicken muscle extract (CMX), and other factors such as choline acetyltransferase development factor (CDF) are potent survival factors for somatic motor neurons (Oppenheim et al., 1988; McManaman et al., 1990; Huang and Reichardt, 2001). By comparison, there are fewer factors identified that promote the survival of visceral motor neurons, including nerve growth factor (NGF) (Oppenheim et al., 1982b) and possibly fibroblast growth factor 1 and 2 (FGF1 and FGF2) (Teng et al., 1998;

Teng et al., 1999). Thus with a smaller repertoire of growth factors and receptors through which they signal as "backups," there may be a greater reliance upon ALK and binding of its ligand for promotion of visceral motor neuron survival – possibly explaining the dramatic decrease in Isl1+ CT motor neurons upon *Alk* knockdown. Since cell death can be induced before the time of PCD in the preganglionic motor neurons (E7 – E10) (Oppenheim et al., 1982a), while their axons have already extended to targets at st 28, ALK may help to keep these neurons alive until later stages when ligand becomes limited and competitive binding begins. This series of potential events provides one possible explanation to an important question: How does ALK promote cell survival?

It is thought that during development an excess of presumptive neurons are generated and then compete for limited trophic factors in local or more distant surrounding areas – as neurons extend their axons, trophic factors available in sufficient quantities signal through their receptor, allowing a cell to survive, while a cell receiving inadequate amounts of trophic factor cannot generate a signal cascade and dies (known as the Neurotrophic Hypothesis). Support for this current view can be observed in the developing spinal cord where 50% of motor neurons generated undergo temporally and spatially specific cell death (Oppenheim 1991). Motor neuron dependence on target-derived trophic factors during development has been well established, with loss of trophic support leading to death in these cells (Li et al., 2001; Newbern et al., 2005). Studies have shown that, in motor neurons, trophic factors prevent apoptosis by signaling through the phosphoinositide-3-kinase (PI3K) pathway and sometimes by way of the extracellular signal-related kinase 1/2 (ERK1/2) pathway (Huang and Reichardt, 2001; Newbern et al., 2005). PI3K activation allows anti-apoptotic Bcl-2

family members to interfere with the generation of a caspase cascade that would result in apoptosis. Activation of the ERK pathway leads to phosphorylation of CREB (cAMP-related enhancer binding protein) which in turn regulates genes whose products are essential for prolonged neurotrophin-dependent survival of neurons (Huang and Reichardt, 2001). ERK1/2 signaling also appears to circumvent cell death by means of Bcl-2 family proteins, but the exact mechanisms are not clear. Since ALK dimerization and signaling via PTN has been shown to initiate signal cascades through the PI3K and ERK1/2 pathways, resulting in cell survival (Bai et al., 2000; Bowden et al., 2002), and *Alk* and *Ptn* have overlapping expression profiles in chick, it is entirely plausible that ALK and its ligand propagate a direct signal for survival in motor neurons.

In addition to the aforementioned scenario, recent studies suggest that electrical excitation, perhaps from activity of nascent synapses, and depolarization by means of acetylcholine receptor activation can increase neuron survival (Pugh and Margiotta, 2000; Moulder et al., 2003). Thus, establishment of stable synapses appears to contribute to neuronal survival and RTKs, including MuSK and ErbB receptors, are known to be involved with synapse formation (Moore et al., 2001). This raises the possibility that ALK is necessary for synaptogenesis and cell death is consequential in motor neurons unable to generate synapses due to *Alk* silencing.

Furthermore, it is possible that ALK contributes to guidance of axons since its reported ligand, pleiotrophin, has been observed in developing axon tracts (Silos-Santiago et al., 1996). Other RTKs, such as the members of the Eph receptor family, are known to influence guidance and show a similar expression profile to *Alk*, being expressed in motor

columns and corresponding target musculature (Kilpatrick et al., 1996; Iwamasa et al., 1999). If involved with axonal guidance, *Alk* knockdown could interfere with correct pathfinding so that axons are unable to reach the proper targets. Without finding the correct targets, axons would potentially be deprived of trophic support and/or the ability to form synapses, indirectly resulting in cell death.

Additionally, it is of importance to address the likely identity of more dorsally located cells undergoing death that are not motor neurons. Based on their position and the fact that glial progenitors, including oligodendrocyte and astrocyte precursors, are restricted to the neuroepithelium during the time of analysis (st 28) (Agius et al., 2004; Braquart-Varnier et al., 2004; Pringle et al., 1998), interneurons are the most logical candidates for the remaining unidentified cells. Interneurons are relatively resistant to induced cell death following removal of targets (MaKay and Oppenheim, 1991); therefore, should immunostaining with specific transcription factor markers identify the unknown dying cells as interneurons, their death can be considered ALK-dependent rather than an after effect caused by concurrent motor neuron death.

Future Direction

In this era of stem cell and tissue regeneration research, identification of ligand/receptor interactions involved in tissue development is of critical importance. The discovery of the receptor tyrosine kinase, anaplastic lymphoma kinase, and its putative ligand, pleiotrophin, promises to be of monumental significance. Our studies indicate that ALK contributes to the development of the central and peripheral nervous systems,

particularly the spinal cord where ALK promotes motor neuron survival. Thus, administration of pleiotrophin after spinal cord injury, possibly in concert with the introduction of neural stem cells at the site of trauma, may prove to be of therapeutic value one day. However, before that day arrives, there remains further study to assess ALK's potential importance.

In the course of future studies, the findings of the experiments presented here need to be corroborated with gain-of-function analyses. Such investigations will require the isolation and sequencing of a full-length chick *Alk* cDNA with subsequent cloning into an expression vector so that receptor will be overexpressed yielding increased ALK activity in cells of the spinal cord. If characterization of a full-length cDNA proves too difficult, then a plasmid encoding a chimeric receptor composed of the intracellular portion of ALK (for which the cDNA sequence is known) fused to the extracellular domain of CD8α could be constructed, producing constitutive signaling through the ALK intracellular domains since the chimera would dimerize autonomously in a ligand-independent fashion. Two days after injection and electroporation into st 22 chick neural tube, the effects of the full-length or chimeric construct would be analyzed by TUNEL assay. If the gain of function is successful and ALK is truly involved with promoting neuronal cell survival, the expected result would be decreased cell death in comparison to the non-electroporated side.

Furthermore, it is of particular interest to investigate whether cell survival is an indirect result of ALK's potential role in axonal guidance or synaptogenesis. For this determination, the U6 promoter and hairpin insert from either pSilencerAlk1 or 2 could be excised and subcloned into a GFP-expressing reporter plasmid such as pMES or pCAGGS.

This strategy allows for direct labeling of axons in motor neurons where *Alk* transcript is silenced. Any adverse effects of *Alk* knockdown on axonal guidance should be visible since axons will be expressing GFP. In comparison to negative controls, pathfinding of axons to targets can be assessed for any abnormalities. In addition, the same embryos can be immunostained for α-bungarotoxin (α-BTX) (present at forming synapses). If *Alk* silencing affects axonal guidance or synaptogenesis negatively, innervation of inappropriate target(s) or decreased α-BTX staining at neuromuscular junctions in the electroporated side of embryos may be observed. These phenotypic changes would suggest that ALK's promotion of cell survival is an indirect consequence of its primary role.

Lastly, it is necessary to determine the functional role of ALK in DRG and SG development through loss and gain-of-function analyses. RNAi-mediated knockdown can be achieved in ovo with injection and electroporation of pSilencerAlk1, pSilencerAlk2, or siALK siRNA into st 10 neural tube. At this stage, neural crest cells have not yet delaminated from the neural tube; therefore, cells giving rise to the DRG and SG are efficiently transfected upon electroporation. In addition, overexpression of either the full-length or chimeric ALK (previously described) in ovo is accomplished by injection and electroporation of construct DNA into st 10 chick neural tube. Two or three days after electroporation, phenotypic changes can be identified and analyzed to assess the impact of *Alk* knockdown or overexpression and to subsequently determine ALK's role in vivo in dorsal root and sympathetic ganglia.

CHAPTER 6

CONCLUSIONS

This thesis has provided an in-depth expression profile for chick that reveals *Alk* mRNA is prominently and distinctly expressed in DRG, SG, spinal cord, and musculature. The period of *Alk* expression coincides with key biological events such as cellular proliferation, neuronal differentiation, programmed cell death, and motor neuron innervation of muscles, indicating ALK's potential role in numerous major developmental processes. Of particular interest are the findings that *Alk* mRNA is present in chick spinal motor neurons during the entire period of programmed cell death, suggesting a potential role for this receptor tyrosine kinase in motor neuron survival. Recent investigations indeed show that *Alk* knockdown by means of in ovo RNAi results in premature neuronal cell death. Thus, this thesis also provides ALK with its first identified function in vivo in the developing nervous system. Future experiments will allow for the elucidation of additional roles for ALK in the peripheral nervous system, specifically the dorsal root and sympathetic ganglia.

LITERATURE CITED

Agius E, Soukkarieh C, Danesin C, Kan P, Takebayashi H, Soula C, Cochard P. 2004. Converse control of oligodendrocyte and astrocyte lineage development by Sonic hedgehog in the chick spinal cord. Dev Biol 270(2):308-321.

Avivi C, Goldstein RS. 1999. Differential expression of Islet-1 in neural crest-derived ganglia: Islet-1 + dorsal root ganglion cells are post-mitotic and Islet-1 + sympathetic ganglion cells are still cycling. Brain Res Dev Brain Res 115(1):89-92.

Bai RY, Ouyang T, Miething C, Morris SW, Peschel C, Duyster J. 2000. Nucleophosmin-anaplastic lymphoma kinase associated with anaplastic large-cell lymphoma activates the phosphatidylinositol 3-kinase/Akt antiapoptotic signaling pathway. Blood 96(13):4319-4327.

Bowden ET, Stoica GE, Wellstein A. 2002. Anti-apoptotic signaling of pleiotrophin through its receptor, anaplastic lymphoma kinase. J Biol Chem 277(39):35862-35868.

Braquart-Varnier C, Danesin C, Clouscard-Martinato C, Agius E, Escalas N, Benazeraf B, Ai X, Emerson C, Cochard P, Soula C. 2004. A subtractive approach to characterize genes with regionalized expression in the gliogenic ventral neuroepithelium: identification of chick sulfatase 1 as a new oligodendrocyte lineage gene. Mol Cell Neurosci 25(4):612-628.

Briscoe J, Ericson J. 1999. The specification of neuronal identity by graded Sonic Hedgehog signalling. Semin Cell Dev Biol 10(3):353-362.

Britsch S, Li L, Kirchhoff S, Theuring F, Brinkmann V, Birchmeier C, Riethmacher D. 1998. The ErbB2 and ErbB3 receptors and their ligand, neuregulin-1, are essential for development of the sympathetic nervous system. Genes Dev 12(12):1825-1836.

Bron R, Eickholt BJ, Vermeren M, Fragale N, Cohen J. 2004. Functional knockdown of neuropilin-1 in the developing chick nervous system by siRNA hairpins phenocopies genetic ablation in the mouse. Dev Dyn 230(2):299-308.

Caplen NJ, Parrish S, Imani F, Fire A, Morgan RA. 2001. Specific inhibition of gene expression by small double-stranded RNAs in invertebrate and vertebrate systems. Proc Natl Acad Sci U S A 98(17):9742-9747.

Carr VM, Simpson SB, Jr. 1978. Proliferative and degenerative events in the early development of chick dorsal root ganglia. I. Normal development. J Comp Neurol 182(4):727-739.

Chesnutt C, Niswander L. 2004. Plasmid-based short-hairpin RNA interference in the chicken embryo. Genesis 39(2):73-78.

Cornbrooks EB, Newton CJ, Forehand CJ. 1997. Development of differential preganglionic projections to pre- and paravertebral sympathetic ganglia. J Comp Neurol 382(1):1-18.

Debby-Brafman A, Burstyn-Cohen T, Klar A, Kalcheim C. 1999. F-Spondin, expressed in somite regions avoided by neural crest cells, mediates inhibition of distinct somite domains to neural crest migration. Neuron 22(3):475-488.

Dreyfus J, Brunet-de Carvalho N, Duprez D, Raulais D, Vigny M. 1998. HB GAM/pleiotrophin: localization of mRNA and protein in the chicken developing leg. Int J Dev Biol 42(2):189-198.

Eickholt BJ, Mackenzie SL, Graham A, Walsh FS, Doherty P. 1999. Evidence for collapsin-1 functioning in the control of neural crest migration in both trunk and hindbrain regions. Development 126(10):2181-2189.

Elbashir SM, Lendeckel W, Tuschl T. 2001. RNA interference is mediated by 21- and 22-nucleotide RNAs. Genes Dev 15(2):188-200.

Elenius K, Jalkanen M. 1994. Function of the syndecans--a family of cell surface proteoglycans. J Cell Sci 107 (Pt 11):2975-2982.

Englund C, Birve A, Falileeva L, Grabbe C, Palmer RH. 2006. Miple1 and miple2 encode a family of MK/PTN homologues in Drosophila melanogaster. Dev Genes Evol 216(1):10-18.

Ericson J, Rashbass P, Schedl A, Brenner-Morton S, Kawakami A, van Heyningen V, Jessell TM, Briscoe J. 1997. Pax6 controls progenitor cell identity and neuronal fate in response to graded Shh signaling. Cell 90(1):169-180.

Fire A, Xu S, Montgomery MK, Kostas SA, Driver SE, Mello CC. 1998. Potent and specific genetic interference by double-stranded RNA in Caenorhabditis elegans. Nature 391(6669):806-811.

Fredette BJ, Ranscht B. 1994. T-cadherin expression delineates specific regions of the developing motor axon-hindlimb projection pathway. J Neurosci 14(12):7331-7346.

Goldstein RS, Kalcheim C. 1991. Normal segmentation and size of the primary sympathetic ganglia depend upon the alternation of rostrocaudal properties of the somites. Development 112(1):327-334.

Gould TW, Oppenheim RW. 2004. The function of neurotrophic factor receptors expressed by the developing adductor motor pool in vivo. J Neurosci 24(19):4668-4682.

Hamburger V, Brunso-Bechtold JK, Yip JW. 1981. Neuronal death in the spinal ganglia of the chick embryo and its reduction by nerve growth factor. J Neurosci 1(1):60-71.

Hamburger V, Hamilton HL. 1992. A series of normal stages in the development of the chick embryo. 1951. Dev Dyn 195(4):231-272.

Hamilton AJ, Baulcombe DC. 1999. A species of small antisense RNA in posttranscriptional gene silencing in plants. Science 286(5441):950-952.

Helms AW, Johnson JE. 2003. Specification of dorsal spinal cord interneurons. Curr Opin Neurobiol 13(1):42-49.

Hollyday M. 1980. Organization of motor pools in the chick lumbar lateral motor column. J Comp Neurol 194(1):143-170.

Hollyday M, Hamburger V. 1977. An autoradiographic study of the formation of the lateral motor column in the chick embryo. Brain Res 132(2):197-208.

Hollyday M, Hamburger V, Farris JM. 1977. Localization of motor neuron pools supplying identified muscles in normal and supernumerary legs of chick embryo. Proc Natl Acad Sci U S A 74(8):3582-3586.

Huang EJ, Reichardt LF. 2001. Neurotrophins: roles in neuronal development and function. Annu Rev Neurosci 24:677-736.

Hubbard SR, Till JH. 2000. Protein tyrosine kinase structure and function. Annu Rev Biochem 69:373-398.

Iwahara T, Fujimoto J, Wen D, Cupples R, Bucay N, Arakawa T, Mori S, Ratzkin B, Yamamoto T. 1997. Molecular characterization of ALK, a receptor tyrosine kinase expressed specifically in the nervous system. Oncogene 14(4):439-449.

Iwamasa H, Ohta K, Yamada T, Ushijima K, Terasaki H, Tanaka H. 1999. Expression of Eph receptor tyrosine kinases and their ligands in chick embryonic motor neurons and hindlimb muscles. Dev Growth Differ 41(6):685-698.

Jessell TM. 2000. Neuronal specification in the spinal cord: inductive signals and transcriptional codes. Nat Rev Genet 1(1):20-29.

Kaplan DR, Miller FD. 2000. Neurotrophin signal transduction in the nervous system. Curr Opin Neurobiol 10(3):381-391.

Kardon G. 1998. Muscle and tendon morphogenesis in the avian hind limb. Development 125(20):4019-4032.

Khvorova A, Reynolds A, Jayasena SD. 2003. Functional siRNAs and miRNAs exhibit strand bias. Cell 115(2):209-216.

Kilpatrick TJ, Brown A, Lai C, Gassmann M, Goulding M, Lemke G. 1996. Expression of the Tyro4/Mek4/Cek4 gene specifically marks a subset of embryonic motor neurons and their muscle targets. Mol Cell Neurosci 7(1):62-74.

Kirby ML, Gilmore SA. 1976. A correlative histofluorescence and light microscopic study of the formation of the sympathetic trunks in chick embryos. Anat Rec 186(3):437-449.

Kojima T, Katsumi A, Yamazaki T, Muramatsu T, Nagasaka T, Ohsumi K, Saito H. 1996. Human ryudocan from endothelium-like cells binds basic fibroblast growth factor, midkine, and tissue factor pathway inhibitor. J Biol Chem 271(10):5914-5920.

Krull CE. 2001. Segmental organization of neural crest migration. Mech Dev 105(1-2):37-45.

Krull CE, Collazo A, Fraser SE, Bronner-Fraser M. 1995. Segmental migration of trunk neural crest: time-lapse analysis reveals a role for PNA-binding molecules. Development 121(11):3733-3743.

Krull CE, Lansford R, Gale NW, Collazo A, Marcelle C, Yancopoulos GD, Fraser SE, Bronner-Fraser M. 1997. Interactions of Eph-related receptors and ligands confer rostrocaudal pattern to trunk neural crest migration. Curr Biol 7(8):571-580.

LaBonne C, Bronner-Fraser M. 1998. Neural crest induction in Xenopus: evidence for a two-signal model. Development 125(13):2403-2414.

Landmesser L. 1978. The distribution of motoneurones supplying chick hind limb muscles. J Physiol 284:371-389.

Landmesser LT. 2001. The acquisition of motoneuron subtype identity and motor circuit formation. Int J Dev Neurosci 19(2):175-182.

Le Douarin NM, Teillet MA. 1974. Experimental analysis of the migration and differentiation of neuroblasts of the autonomic nervous system and of neurectodermal mesenchymal derivatives, using a biological cell marking technique. Dev Biol 41(1):162-184.

Lee HH, Norris A, Weiss JB, Frasch M. 2003. Jelly belly protein activates the receptor tyrosine kinase Alk to specify visceral muscle pioneers. Nature 425(6957):507-512.

Lee MK, Tuttle JB, Rebhun LI, Cleveland DW, Frankfurter A. 1990. The expression and posttranslational modification of a neuron-specific beta-tubulin isotype during chick embryogenesis. Cell Motil Cytoskeleton 17(2):118-132.

Lee SK, Pfaff SL. 2001. Transcriptional networks regulating neuronal identity in the developing spinal cord. Nat Neurosci 4 Suppl:1183-1191.

Li L, Oppenheim RW, Milligan CE. 2001. Characterization of the execution pathway of developing motoneurons deprived of trophic support. J Neurobiol 46(4):249-264.

Liao EH, Hung W, Abrams B, Zhen M. 2004. An SCF-like ubiquitin ligase complex that controls presynaptic differentiation. Nature 430(6997):345-350.

Liem KF, Jr., Tremml G, Jessell TM. 1997. A role for the roof plate and its resident TGFbeta-related proteins in neuronal patterning in the dorsal spinal cord. Cell 91(1):127-138.

Lin JH, Saito T, Anderson DJ, Lance-Jones C, Jessell TM, Arber S. 1998. Functionally related motor neuron pool and muscle sensory afferent subtypes defined by coordinate ETS gene expression. Cell 95(3):393-407.

Loren CE, Englund C, Grabbe C, Hallberg B, Hunter T, Palmer RH. 2003. A crucial role for the Anaplastic lymphoma kinase receptor tyrosine kinase in gut development in Drosophila melanogaster. EMBO Rep.

Loren CE, Scully A, Grabbe C, Edeen PT, Thomas J, McKeown M, Hunter T, Palmer RH. 2001. Identification and characterization of DAlk: a novel Drosophila melanogaster RTK which drives ERK activation in vivo. Genes Cells 6(6):531-544.

Maeda N, Ichihara-Tanaka K, Kimura T, Kadomatsu K, Muramatsu T, Noda M. 1999. A receptor-like protein-tyrosine phosphatase PTPzeta/RPTPbeta binds a heparin-binding growth factor midkine. Involvement of arginine 78 of midkine in the high affinity binding to PTPzeta. J Biol Chem 274(18):12474-12479.

Maeda N, Nishiwaki T, Shintani T, Hamanaka H, Noda M. 1996. 6B4 proteoglycan/phosphacan, an extracellular variant of receptor-like protein-tyrosine phosphatase zeta/RPTPbeta, binds pleiotrophin/heparin-binding growth-associated molecule (HB-GAM). J Biol Chem 271(35):21446-21452.

McKay SE, Oppenheim RW. 1991. Lack of evidence for cell death among avian spinal cord interneurons during normal development and following removal of targets and afferents. J Neurobiol 22(7):721-733.

McLennan R, Krull CE. 2002. Ephrin-as cooperate with EphA4 to promote trunk neural crest migration. Gene Expr 10(5-6):295-305.

McManaman JL, Oppenheim RW, Prevette D, Marchetti D. 1990. Rescue of motoneurons from cell death by a purified skeletal muscle polypeptide: effects of the ChAT development factor, CDF. Neuron 4(6):891-898.

Minks MA, West DK, Benvin S, Baglioni C. 1979. Structural requirements of double-stranded RNA for the activation of 2',5'-oligo(A) polymerase and protein kinase of interferon-treated HeLa cells. J Biol Chem 254(20):10180-10183.

Moore C, Leu M, Muller U, Brenner HR. 2001. Induction of multiple signaling loops by MuSK during neuromuscular synapse formation. Proc Natl Acad Sci U S A 98(25):14655-14660.

Moran-Rivard L, Kagawa T, Saueressig H, Gross MK, Burrill J, Goulding M. 2001. Evx1 is a postmitotic determinant of v0 interneuron identity in the spinal cord. Neuron 29(2):385-399.

Morris SW, Naeve C, Mathew P, James PL, Kirstein MN, Cui X, Witte DP. 1997. ALK, the chromosome 2 gene locus altered by the t(2;5) in non-Hodgkin's lymphoma, encodes a novel neural receptor tyrosine kinase that is highly related to leukocyte tyrosine kinase (LTK). Oncogene 14(18):2175-2188.

Motegi A, Fujimoto J, Kotani M, Sakuraba H, Yamamoto T. 2004. ALK receptor tyrosine kinase promotes cell growth and neurite outgrowth. J Cell Sci 117(Pt 15):3319-3329.

Moulder KL, Cormier RJ, Shute AA, Zorumski CF, Mennerick S. 2003. Homeostatic effects of depolarization on Ca2+ influx, synaptic signaling, and survival. J Neurosci 23(5):1825-1831.

Napoli C, Lemieux C, Jorgensen R. 1990. Introduction of a Chimeric Chalcone Synthase Gene into Petunia Results in Reversible Co-Suppression of Homologous Genes in trans. Plant Cell 2(4):279-289.

Newbern J, Taylor A, Robinson M, Li L, Milligan CE. 2005. Decreases in phosphoinositide-3-kinase/Akt and extracellular signal-regulated kinase 1/2 signaling activate components of spinal motoneuron death. J Neurochem 94(6):1652-1665.

Nieto MA, Patel K, Wilkinson DG. 1996. In situ hybridization analysis of chick embryos in whole mount and tissue sections. Methods Cell Biol 51:219-235.

Nieto MA, Sargent MG, Wilkinson DG, Cooke J. 1994. Control of cell behavior during vertebrate development by Slug, a zinc finger gene. Science 264(5160):835-839.

Nolo R, Kaksonen M, Rauvala H. 1996. Developmentally regulated neurite outgrowth response from dorsal root ganglion neurons to heparin-binding growth-associated molecule (HB-GAM) and the expression of HB-GAM in the targets of the developing dorsal root ganglion neurites. Eur J Neurosci 8(8):1658-1665.

Okado N, Oppenheim RW. 1984. Cell death of motoneurons in the chick embryo spinal cord. IX. The loss of motoneurons following removal of afferent inputs. J Neurosci 4(6):1639-1652.

Oppenheim RW. 1991. Cell death during development of the nervous system. Annu Rev Neurosci 14:453-501.

Oppenheim RW, Haverkamp LJ, Prevette D, McManaman JL, Appel SH. 1988. Reduction of naturally occurring motoneuron death in vivo by a target-derived neurotrophic factor. Science 240(4854):919-922.

Oppenheim RW, Maderdrut JL, Wells DJ. 1982a. Cell death of motoneurons in the chick embryo spinal cord. VI. Reduction of naturally occurring cell death in the thoracolumbar column of Terni by nerve growth factor. J Comp Neurol 210(2):174-189.

Oppenheim RW, Maderdrut JL, Wells DJ. 1982b. Reduction of naturally-occurring cell death in the thoraco-lumbar preganglionic cell column of the chick embryo by nerve growth factor and hemicholinium-3. Brain Res 255(1):134-139.

Paddison PJ, Caudy AA, Bernstein E, Hannon GJ, Conklin DS. 2002. Short hairpin RNAs (shRNAs) induce sequence-specific silencing in mammalian cells. Genes Dev 16(8):948-958.

Pekarik V, Bourikas D, Miglino N, Joset P, Preiswerk S, Stoeckli ET. 2003. Screening for gene function in chicken embryo using RNAi and electroporation. Nat Biotechnol 21(1):93-96.

Piccinini G, Bacchiocchi R, Serresi M, Vivani C, Rossetti S, Gennaretti C, Carbonari D, Fazioli F. 2002. A ligand-inducible epidermal growth factor receptor/anaplastic lymphoma kinase chimera promotes mitogenesis and transforming properties in 3T3 cells. J Biol Chem 277(25):22231-22239.

Powers C, Aigner A, Stoica GE, McDonnell K, Wellstein A. 2002. Pleiotrophin signaling through anaplastic lymphoma kinase is rate-limiting for glioblastoma growth. J Biol Chem 277(16):14153-14158.

Prasad A, Hollyday M. 1991. Development and migration of avian sympathetic preganglionic neurons. J Comp Neurol 307(2):237-258.

Pringle NP, Guthrie S, Lumsden A, Richardson WD. 1998. Dorsal spinal cord neuroepithelium generates astrocytes but not oligodendrocytes. Neuron 20(5):883-893.

Pugh PC, Margiotta JF. 2000. Nicotinic acetylcholine receptor agonists promote survival and reduce apoptosis of chick ciliary ganglion neurons. Mol Cell Neurosci 15(2):113-122.

Pulford K, Morris SW, Turturro F. 2004. Anaplastic lymphoma kinase proteins in growth control and cancer. J Cell Physiol 199(3):330-358.

Ranscht B, Bronner-Fraser M. 1991. T-cadherin expression alternates with migrating neural crest cells in the trunk of the avian embryo. Development 111(1):15-22.

Rao M, Baraban JH, Rajaii F, Sockanathan S. 2004. In vivo comparative study of RNAi methodologies by in ovo electroporation in the chick embryo. Dev Dyn 231(3):592-600.

Rao M, Sockanathan S. 2005. Transmembrane protein GDE2 induces motor neuron differentiation in vivo. Science 309(5744):2212-2215.

Reissmann E, Ernsberger U, Francis-West PH, Rueger D, Brickell PM, Rohrer H. 1996. Involvement of bone morphogenetic protein-4 and bone morphogenetic protein-7 in the differentiation of the adrenergic phenotype in developing sympathetic neurons. Development 122(7):2079-2088.

Reynolds A, Leake D, Boese Q, Scaringe S, Marshall WS, Khvorova A. 2004. Rational siRNA design for RNA interference. Nat Biotechnol 22(3):326-330.

Rickmann M, Fawcett JW, Keynes RJ. 1985. The migration of neural crest cells and the growth of motor axons through the rostral half of the chick somite. J Embryol Exp Morphol 90:437-455.

Rifkin JT, Todd VJ, Anderson LW, Lefcort F. 2000. Dynamic expression of neurotrophin receptors during sensory neuron genesis and differentiation. Dev Biol 227(2):465-480.

Roelink H, Porter JA, Chiang C, Tanabe Y, Chang DT, Beachy PA, Jessell TM. 1995. Floor plate and motor neuron induction by different concentrations of the amino-terminal cleavage product of sonic hedgehog autoproteolysis. Cell 81(3):445-455.

Rothman TP, Gershon MD, Holtzer H. 1978. The relationship of cell division to the acquisition of adrenergic characteristics by developing sympathetic ganglion cell precursors. Dev Biol 65(2):322-341.

Saueressig H, Burrill J, Goulding M. 1999. Engrailed-1 and netrin-1 regulate axon pathfinding by association interneurons that project to motor neurons. Development 126(19):4201-4212.

Schlessinger J. 2000. Cell signaling by receptor tyrosine kinases. Cell 103(2):211-225.

Schneider C, Wicht H, Enderich J, Wegner M, Rohrer H. 1999. Bone morphogenetic proteins are required in vivo for the generation of sympathetic neurons. Neuron 24(4):861-870.

Sharma K, Leonard AE, Lettieri K, Pfaff SL. 2000. Genetic and epigenetic mechanisms contribute to motor neuron pathfinding. Nature 406(6795):515-519.

Sharma K, Sheng HZ, Lettieri K, Li H, Karavanov A, Potter S, Westphal H, Pfaff SL. 1998. LIM homeodomain factors Lhx3 and Lhx4 assign subtype identities for motor neurons. Cell 95(6):817-828.

Shepherd I, Luo Y, Raper JA, Chang S. 1996. The distribution of collapsin-1 mRNA in the developing chick nervous system. Dev Biol 173(1):185-199.

Shiota M, Fujimoto J, Semba T, Satoh H, Yamamoto T, Mori S. 1994. Hyperphosphorylation of a novel 80 kDa protein-tyrosine kinase similar to Ltk in a human Ki-1 lymphoma cell line, AMS3. Oncogene 9(6):1567-1574.

Shirasaki R, Pfaff SL. 2002. Transcriptional codes and the control of neuronal identity. Annu Rev Neurosci 25:251-281.

Silos-Santiago I, Yeh HJ, Gurrieri MA, Guillerman RP, Li YS, Wolf J, Snider W, Deuel TF. 1996. Localization of pleiotrophin and its mRNA in subpopulations of neurons and their corresponding axonal tracts suggests important roles in neural-glial interactions during development and in maturity. J Neurobiol 31(3):283-296.

Smet P, Rush RA, Straznicky C. 1986. The thoracic sympathetic neurons of the chick: normal development and the effects of nerve growth factor. Histol Histopathol 1(4):315-322.

Smith CJ, Watson CF, Bird CR, Ray J, Schuch W, Grierson D. 1990. Expression of a truncated tomato polygalacturonase gene inhibits expression of the endogenous gene in transgenic plants. Mol Gen Genet 224(3):477-481.

Sockanathan S, Perlmann T, Jessell TM. 2003. Retinoid receptor signaling in postmitotic motor neurons regulates rostrocaudal positional identity and axonal projection pattern. Neuron 40(1):97-111.

Souttou B, Carvalho NB, Raulais D, Vigny M. 2001. Activation of anaplastic lymphoma kinase receptor tyrosine kinase induces neuronal differentiation through the mitogen-activated protein kinase pathway. J Biol Chem 276(12):9526-9531.

Stoica GE, Kuo A, Aigner A, Sunitha I, Souttou B, Malerczyk C, Caughey DJ, Wen D, Karavanov A, Riegel AT, Wellstein A. 2001. Identification of anaplastic lymphoma kinase as a receptor for the growth factor pleiotrophin. J Biol Chem 276(20):16772-16779.

Stoica GE, Kuo A, Powers C, Bowden ET, Sale EB, Riegel AT, Wellstein A. 2002. Midkine binds to anaplastic lymphoma kinase (ALK) and acts as a growth factor for different cell types. J Biol Chem 277(39):35990-35998.

Tanabe Y, William C, Jessell TM. 1998. Specification of motor neuron identity by the MNR2 homeodomain protein. Cell 95(1):67-80.

Taxman DJ, Livingstone LR, Zhang J, Conti BJ, Iocca HA, Williams KL, Lich JD, Ting JP, Reed W. 2006. Criteria for effective design, construction, and gene knockdown by shRNA vectors. BMC Biotechnol 6:7.

Tello, J.F. 1925. Sobre la formacion de los ganglios nerviosos craneales y el mesectodermo cefalico en los embriones de pollo. Trab Inst Cajal Invest Biol. 38: 1-40.

Teng YD, Mocchetti I, Taveira-DaSilva AM, Gillis RA, Wrathall JR. 1999. Basic fibroblast growth factor increases long-term survival of spinal motor neurons and improves respiratory function after experimental spinal cord injury. J Neurosci 19(16):7037-7047.

Teng YD, Mocchetti I, Wrathall JR. 1998. Basic and acidic fibroblast growth factors protect spinal motor neurones in vivo after experimental spinal cord injury. Eur J Neurosci 10(2):798-802.

Tijsterman M, Ketting RF, Plasterk RH. 2002. The genetics of RNA silencing. Annu Rev Genet 36:489-519.

Tsuchida T, Ensini M, Morton SB, Baldassare M, Edlund T, Jessell TM, Pfaff SL. 1994. Topographic organization of embryonic motor neurons defined by expression of LIM homeobox genes. Cell 79(6):957-970.

Tuschl T, Zamore PD, Lehmann R, Bartel DP, Sharp PA. 1999. Targeted mRNA degradation by double-stranded RNA in vitro. Genes Dev 13(24):3191-3197.

van der Krol AR, Mur LA, Beld M, Mol JN, Stuitje AR. 1990. Flavonoid genes in petunia: addition of a limited number of gene copies may lead to a suppression of gene expression. Plant Cell 2(4):291-299.

Wakamatsu Y, Watanabe Y, Nakamura H, Kondoh H. 1997. Regulation of the neural crest cell fate by N-myc: promotion of ventral migration and neuronal differentiation. Development 124(10):1953-1962.

Wang HU, Anderson DJ. 1997. Eph family transmembrane ligands can mediate repulsive guidance of trunk neural crest migration and motor axon outgrowth. Neuron 18(3):383-396.

Wilkinson DG, Nieto MA. 1993. Detection of messenger RNA by in situ hybridization to tissue sections and whole mounts. Methods Enzymol 225:361-373.

William CM, Tanabe Y, Jessell TM. 2003. Regulation of motor neuron subtype identity by repressor activity of Mnx class homeodomain proteins. Development 130(8):1523-1536.

Zhuang B, Sockanathan S. 2006. Dorsal-ventral patterning: a view from the top. Curr Opin Neurobiol 16(1):20-24.

APPENDICES

APPENDIX A

α-ALK ANTIBODY STAINING

Observations

Antibody Used	Stage	Observed Slide Staining – Transverse Sections (14 μm)
PI	25	No Staining
4817	25	Ubiquitous punctate staining in mitotic & postmitotic cells
4841	25	Axial muscles, margins of SC, inner core (not perimeter) of DRG
DAKO	25	No signal in DRG or SC, possible signal in SG
PI	35	Possibly stains DRG neurons and SG neurons
DAKO	35	Stains motor neurons and DRG
4817	35	Stains filamentous protein in all cells
4841	35	No staining of DRG, faint staining of MNs, stains muscle
PI	36	Stains SG and DRG (large diameter) neurons, no SC staining
DAKO	36	No signal in DRG or SC
4817	36	Stains DRG, SG, & MNs (no punctate staining)
4841	36	No DRG staining, weak in SG, punctate stain in SC & muscle stain
PI	38	Stains DRG, SG & SC diffusely, but greater than background
DAKO	38	Stains DRG, SG – strongly; MNs - weakly
4817	38	Strong staining of DRG and SG (not on axons)
4841	38	No DRG/SG staining; punctate staining all over – strong in muscle
Zymed	24	Stains DRG axons, MNs, and SG
Zymed	35	Stains ventral portion of SC, DRG (axons and some cells), SG (axons coursing through, but cell bodies aren't stained, intercostal muscles

PI = Pre-immune IgG
4817 = Our rabbit polyclonal α-ALK antibody #1 (rabbit anti-chick)*
4841 = Our rabbit polyclonal α-ALK antibody #2 (rabbit anti-chick)*
DAKO = Mouse monoclonal α-ALK antibody from Dako Cytochemical (mouse anti-human)**
Zymed = Rabbit polyclonal α-ALK antibody from Zymed Laboratories (rabbit anti-human)***
DRG = Dorsal Root Ganglia
SG = Sympathetic Ganglia
SC = Spinal Cord
MNs = Motor Neurons

* - chick polypeptide sequence, corresponding to a.a. 1386-1509 in human ALK, was recombinantly expressed in *E. coli*, purified and used to immunize two different rabbits (#4817 & #4841)
** - human polypeptide sequence, a.a. 1359-1460 from human ALK – possessing ~70% identity and ~85% homology to chick ALK, was recombinantly expressed and used to immunize mice
*** - human polypeptide sequence, a.a. 1366-1468 from human ALK – possessing ~65% identity and ~83% homology to chick ALK, was recombinantly expressed and used to immunize rabbits

Since none of the antibodies provided a staining profile that was a definitive match to in situ hybridization profiling for transcript, in addition to possible recognition by pre-immune IgG, we concluded our results were too ambiguous to warrant further IHC experiments. Presently, use of these antibodies for IHC staining has been placed on hold, however, it may be prudent to further investigate use of certain antibodies that appeared to recognize specific neuron subpopulations more consistently (e.g. 4841 or Zymed pAb for MN staining).

APPENDIX B

STATISTICAL DATA

Statistical Analysis: Student's t-test (one-tailed) – using StatDisk 10.1.0

Ratio of TUNEL+ Cells in spinal cord - # in Electroporated Half:# in Non-electro. Half

Treatment	n	Sample mean	Standard dev.	P value for claim: exp. > control
pMES	3	1.136	0.110	
pSilencerAlk1	5	2.31	0.376	0.0011
pSilencerAlk2	5	3.068	0.345	0.0000

Ratio of TUNEL+ Cells in spinal cord - # in Electroporated Half:# in Non-electro. Half

Treatment	n	Sample mean	Standard dev.	P value for claim: exp. > control
DsRed siRNA	3	1.0477	0.160	
siALK siRNA	4	1.36	0.138	0.0196

Ratio of Isl+ CT MNs in spinal cord - # in Electroporated Half:# in Non-electro. Half

Treatment	n	Sample mean	Standard dev.	P value for claim: exp. < control
pMES	2	0.997	0.034	
pSilencerAlk2	3	0.376	0.075	0.0009